https://doi.org/10.1093/plphys/kiad121 PLANT PHYSIOLOGY 2023: 192: 982–999

Plant Physiology®

Research Article

Kiwifruit bZIP transcription factor *AcePosF21* elicits ascorbic acid biosynthesis during cold stress

Xiaoying Liu,[1,2] **Sean M. Bulley**,[3] **Erika Varkonyi-Gasic**,[4] **Caihong Zhong**[1,*] **and Dawei Li**[1,*]

1 Wuhan Botanical Garden, Chinese Academy of Sciences, Jiufeng 1 Road, Wuhan 430074, Hubei, China
2 College of Life Sciences, University of Chinese Academy of Sciences, 19A Yuquan Road, Beijing 100049, China
3 The New Zealand Institute for Plant and Food Research Limited, Private Bag 11600, Palmerston North 4442, New Zealand
4 The New Zealand Institute for Plant and Food Research Limited, Private Bag 92169, Auckland 1142, New Zealand

*Author for correspondence: lidawei@wbgcas.cn (D. L.), caihongzhong@wbgcas.cn (C. Z.)
D.L. and C.Z. planned and designed the research; X.L., C.Z., and D.L. performed experiments and conducted fieldwork; X.L., S.M.B., E.V.G., and D.L. analyzed data; and D.L., X.L., E.V.G., and S.M.B. wrote the manuscript.
The author responsible for distribution of materials integral to the findings presented in this article in accordance with the policy described in the Instructions for Authors (https://academic.oup.com/plphys/pages/general-instructions) is: Dawei Li (lidawei@wbgcas.cn).

Abstract

Cold stress seriously affects plant development, resulting in heavy agricultural losses. L-ascorbic acid (AsA, vitamin C) is an antioxidant implicated in abiotic stress tolerance and metabolism of reactive oxygen species (ROS). Understanding whether and how cold stress elicits AsA biosynthesis to reduce oxidative damage is important for developing cold-resistant plants. Here, we show that the accumulation of AsA in response to cold stress is a common mechanism conserved across the plant kingdom, from single-cell algae to angiosperms. We identified a basic leucine zipper domain (bZIP) transcription factor (TF) of kiwifruit (*Actinidia eriantha* Benth.), AcePosF21, which was triggered by cold and is involved in the regulation of kiwifruit AsA biosynthesis and defense responses against cold stress. AcePosF21 interacted with the R2R3-MYB TF AceMYB102 and directly bound to the promoter of the gene encoding *GDP-L-galactose phosphorylase 3* (*AceGGP3*), a key conduit for regulating AsA biosynthesis, to up-regulate *AceGGP3* expression and produce more AsA, which neutralized the excess ROS induced by cold stress. On the contrary, VIGS or CRISPR-Cas9-mediated editing of *AcePosF21* decreased AsA content and increased the generation of ROS in kiwifruit under cold stress. Taken together, we illustrated a model for the regulatory mechanism of *AcePosF21*-mediated regulation of *AceGGP3* expression and AsA biosynthesis to reduce oxidative damage by cold stress, which provides valuable clues for manipulating the cold resistance of kiwifruit.

Introduction

Abiotic stresses have a devastating effect on plant growth and development, substantially reducing crop yields (Nadarajah 2020). The frequency, intensity, and negative impact of abiotic stresses are predicted to increase with the changing climate and extreme weather conditions, such as unseasonably warm or cold temperatures (Coffel et al. 2016). Cold is a damaging abiotic stress that triggers morphological, physiological, and biochemical changes in plants. At the cellular level, damage from cold stress incorporates disruption of plasma membrane structure, protein denaturation, and production of ROS (Ruelland et al. 2009). ROS act as the key signaling molecules that enable cells to respond quickly to different stimuli (Mittler et al. 2022). Excessive accumulation of ROS leads to oxidative damage that inhibits plant growth and development and reduces plant production (Rivero et al. 2001; Suzuki and Mittler 2006). To minimize the negative effects of cold stress, plant cells have evolved a complex homeostasis system, which includes the production of protective compounds, e.g. maltose (Peng et al. 2014), starch (Liu et al. 2020, 2021), and sucrose (Dahro

Received October 17, 2022. Accepted January 27, 2023. Advance access publication February 24, 2023

et al. 2022). L-ascorbic acid (AsA, vitamin C) is one of the universal nonenzymatic antioxidants having a substantial ROS scavenging potential and affecting many of the fundamental functions in plants (Smirnoff 2011). Exogenous AsA could induce chilling tolerance in tomato (*Solanum lycopersicum* L.), banana (*Musa nana* Lour.), and spinach (*Spinacia oleracea* L.) through the increase in proline, chlorophyll, total phenolic, and flavonoid contents, as well as enriching activities of antioxidant enzymes and expression of molecular chaperones (Lo'Ay and El-Khateeb 2018; Elkelish et al. 2020; Min et al. 2020). It is, however, still unclear how and when plants synthesize AsA to neutralize ROS and respond to cold stress.

A detailed understanding of the cold tolerance mechanisms and molecular regulation of AsA metabolism and ROS scavenging would be beneficial for developing crops more resilient to cold and other abiotic stresses. In the 1960s, wheat (*Triticum aestivum* L.) breeders discovered that the AsA content of winter wheat varieties was considerably higher at the hardening temperature of 1.5 °C than at temperatures ranging between 5 °C and 20 °C (Andrews and Roberts 1961). The AsA and ascorbate peroxidase activities were subsequently confirmed to be associated with the establishment of cold hardiness in tomatoes, beans [*Glycine max* (Linn.) Merr.], coniferous trees [*Cedrus deodara* (Roxb.) G. Don] and winter rape (*Brassica napus* L.) (Michniewicz and Kentzer 1965; Matsko 1967; Doru and Akirlar 2020), suggesting that the cold-induced accumulation of AsA and AsA-mediated cold tolerance may be conserved between different plant species. Determining the critical genes and regulatory pathways in AsA metabolism affected by cold stress will allow a better understanding of how plants strengthen cold hardiness by actively generating antioxidant AsA. The Smirnoff–Wheeler pathway (or D-mannose/L-galactose pathway) predominates in plants (Wheeler et al. 1998). Within this pathway, AsA concentrations in the cell are regulated mainly through the control of transcription and translation of genes encoding *GDP-L-galactose phosphorylase* (*GGP*), although *GDP-mannose pyrophosphorylase* (*GMP*), *GDP-D-mannose-3′, 5′-epimerase* (*GME*), and *L-galactono-1,4-lactone dehydrogenase* (*GLDH*) also contributes to a lesser extent (Wheeler et al. 1998; Laing et al. 2004, 2015; Bulley and Laing 2016; Fenech et al. 2021). However, the key transcription factors (TFs) controlling AsA accumulation in response to cold stress remain unknown.

Multiple TFs have been implicated in cold stress response. MYB TFs have a role in resistance to multiple abiotic and biotic stresses (Li et al. 2019a, 2019b) and members of the bZIP family are crucial for mediating abiotic stress responses (Fujita et al. 2011; Hwang et al. 2014; Yoshida et al. 2015). For example, genes encoding bZIP proteins were strongly upregulated by cold stress in radish (*Rhaphanus sativus*) roots and bananas (Ito et al. 1999; Shekhawat and Ganapathi 2014). In wheat, the transgenic line overexpressing *TabZIP* had improved tolerance to salinity, drought, heat, and oxidative stress (Agarwal et al. 2019). In rice (*Oryza sativa* L.), *OsbZIP16* (Lu et al. 2009), and *OsbZIP23* (Xiang et al. 2008) heightened drought tolerance through an ABA-related pathway, whereas *bZIP73* controlled rice cold tolerance at the reproductive stage to adjust to cold climates (Liu et al. 2018a, 2018b; Liu et al. 2019). The *Arabidopsis AtbZIP1* binds to an ABRE-acting element and coordinates the cold stress response in plants via an ABA-dependent signaling pathway (Sun et al. 2011).

In this study, we identify the key components of the regulatory pathways conferring cold-induced AsA accumulation and reducing oxidative damage by cold stress. We demonstrate that AsA accumulation in response to cold is universally conserved across the plant kingdom and occurs in multiple tissue types. To study the regulation of cold-induced AsA accumulation and action, we focus on a fruit tree with exceptionally high AsA content, namely, *Actinidia eriantha* (kiwifruit), which was usually grown in subtropical climates and vulnerable to freezing damage. We correlate the expression of the key AsA synthesis gene, *GDP-L-galactose phosphorylase-3* (*GGP3*), with ROS scavenging and perform a transcriptomic study to identify genes implicated in AsA-mediated cold tolerance. Herein we report the identification of a bZIP TF named *A. eriantha* PosF21 (*AcePosF21*), which interacts with MYB102 to promote the synthesis of AsA, providing evidence that AsA endows plants with reduced oxidative damage during cold stress.

Results

Cold stress-induced accumulation of ascorbic acid, which alleviated ROS damage

Ascorbic acid, a potent antioxidant with the ability to scavenge free radicals and ROS, has been implicated in cold stress resistance in plants (Cai et al. 2015; Wang et al. 2021). To establish if cold-induced AsA accumulation is widely conserved, we studied cold response in species representing the major clades and subclades in the plant kingdom, namely *Chlamydomonas reinhardtii* (alga), *Physcomitrium patens* (Hedw.) Mitt. (nonvascular land plant), *Azolla imbricata* (Roxb. Ex Griff.) Nakai (fern), *Taxus chinensis* (Pilg.) Rehder (gymnosperm), and six angiosperm species: *Triticum aestivum* L. (monocot), *Nelumbo nucifera* Gaertn. cv. Xiaozilian, *Arabidopsis thaliana* (L.) Heynh. and *Brassica napus* L. in the rosid clade of eudicots, and *Actinidia eriantha* Benth. (kiwifruit), *Nicotiana benthamiana*, and *Solanum lycopersicum* L. cv. Micro-Tom (tomato), representing the asterid clade of eudicots (Fig. 1A). The AsA content of the harvested tissues of plant species varied, ranging from 2.8 to 9457.5 μg/g FW, with kiwifruit being the highest and *A. imbricata* the lowest (Fig. 1B). Except for *A. imbricata*, the majority of plant species showed an elevated AsA accumulation after 4 °C treatments, with increases ranging between 14.4% and 167.5% in vegetative samples and a similar increase in tomato and kiwifruit fruit under cold stress. Notably, AsA accumulation rates differed significantly among plant species. For example, those of *C. reinhardtii*, *B. napus*, *A. thaliana*, and kiwifruit reached the peak value at 6 h, while that of *T. chinensis*, *T. aestivum*, and *N. nucifera* peaked at 2 d (Fig. 1B).

To determine whether higher AsA concentrations could alleviate ROS damage, kiwifruit materials with identical characters except for AsA differences were evaluated under cold stress (4 °C, 6 h). Here, we chose two overexpressed (*OE14* and *OE20*) and two gene-edited lines (*KO13* and *KO15*) from our previous study (Liu et al. 2022), with a 20 to 22-fold increase and a 5 to 6-fold decrease in AsA content compared to wild-type (WT), respectively (Fig. 1C and Supplemental Fig. S1). The ROS content increased in low AsA lines (*KO13* and *KO15*) compared to wild-type and high AsA lines (*OE14* and *OE20*) after cold treatment for 6 h, inferring that higher AsA content is beneficial for scavenging excess ROS in kiwifruit (Fig. 1D). Enhanced NBT and DAB staining (Supplemental Fig. S2A) and two major components of ROS, H_2O_2, and $O_2^{\cdot-}$ were quantified, revealing a significantly lower content in the overexpressed plants than in the WT and gene-edited lines at cold stress (Supplemental Fig. S1, E and F). These results showed that the transgenic plants with higher AsA concentration accumulated less ROS than the WT and that AsA deficiency resulted in higher ROS accumulation in response to cold treatment. This was further supported by higher proline content in *OE14* and *OE20* lines, with corresponding lower proline content in gene-edited mutants (Fig. 1G). Cytosolic proline is an important factor in the freezing tolerance of nonacclimated plants (Hoermiller et al. 2022), whilst electrolyte leakage (EL) and malondialdehyde (MDA) levels indicate cellular injury. The levels of EL and MDA in the high AsA overexpression lines were significantly lower relative to the WT and gene-edited samples exposed to cold (Supplemental Fig. S1, H and I), suggesting that cell injury was lower in the transgenic lines with higher AsA concentrations. The fresh weight of *OE14* and *OE20* was higher during low-temperature conditions, which indicates that increased endogenous AsA reduces cold stress injuries (Supplemental Fig. S2B). In addition, exogenous AsA also restored ROS damage in *KO13* and *KO15* (Supplemental Fig. S3). These results further highlight the importance of AsA in scavenging ROS in plants.

Identification and characterization of cold-responsive AcePosF21 in kiwifruit

To better understand how cold stress triggers AsA biosynthesis, transcriptomic profiles of kiwifruit grown at 25 °C (RT, room temperature) and exposed to 4 °C for 6 h (COLD) were compared. Data stability and accuracy are illustrated by a number of summary statistics, including the number of reads, reads quality, the mapped rate, and principal component analysis (PCA) (Supplemental Fig. S4A and Supplemental Table S1). A total of 5,677 (2,818 down- and 2,859 up-) differentially expressed genes (DEGs) were identified (Supplemental Fig. S4, B and S4C). Gene Ontology (GO) analysis revealed that the DEGs were enriched in stress and chemical response categories (up-regulate, Fig. 2A), and secondary metabolic processes (down-regulate, Fig. 2B). Cold treatment up-regulated the expression levels of *GDP-L-galactose phosphorylase* (*AceGGP*), and *GDP-mannose pyrophosphorylase* (*AceGMP*) in L-galactose pathways of kiwifruit AsA biosynthesis (Fig. 2C). As a key conduit for regulating AsA biosynthesis (Liu et al. 2022), *DTZ79_29g10040* gene (*AceGGP3*) showed a substantially higher expression level in COLD than that of RT (Fig. 2C). To confirm that the accumulation of *AceGGP3* transcript was induced by cold stress, histochemical staining, and a relative expression assay was carried out in transgenic calli exposed to low-temperature. First, *AceGGP3* expression of kiwifruit calli and fruits was clearly increased (Fig. 2D; Supplemental Fig. S5A) under cold treatment, as well as ascorbic acid concentration (176% increase in calli and 42% in fruits) (Fig. 2E; Supplemental Fig. S5B), and there was a significant positive correlation between AsA content and expression of *AceGGP3* ($r = 0.95$ in calli, $r = 0.88$ in fruits) both in calli and fruits (Supplemental Fig. S5, C and S5D). In addition, the intensity of the blue color and β-glucuronidase (GUS) activity was much increased in calli with the *AceGGP3::GUS* construct under cold stress compared with the control (Fig. 2F; Supplemental Fig. S6). Similarly, the expression of the LUC gene driven by the *AceGGP3* promoter in the Dual-LUC reporter assay rose sharply under cold stress (Supplemental Fig. S7), implying that the activity of the *AceGGP3* promoter was activated by cold stress.

To identify the regulatory genes responsible for the up-regulation of *AceGGP3* under cold stress, the transcriptomic profiles, gene expression of cold treatment, and GUS activity assays were conducted. A transcript *DTZ79_07g00850* (*AcePosF21*), whose expression was induced by cold stress (Fig. 2C and Fig. 3A), was positively correlated with the *AceGGP3* expression ($r = 0.64$) and AsA accumulation ($r = 0.71$) (Supplemental Fig. S3, B and C). It encoded a basic leucine zipper (bZIP) domain protein that was 85% similar to CsPosF21 from *Camellia sinensis* (Supplemental Fig. S8), and thus we named it AcePosF21. AcePosF21 was exclusively located in the nucleus (Supplemental Fig. S9) and was able to act in transcriptional activation (Supplemental Fig. S10). Cold-induced up-regulation of *AcePosF21* was also detected in fruits, with transcript accumulation starting at 2 h after cold treatment (Supplemental Fig. S11). Elevated expression in response to cold occurred via transcriptional activation of the *AcePosF21* promoter, demonstrated using infiltration of transcriptional fusion constructs with reporter genes (*AcePosF21::GUS* and *AcePosF21::LUC*) in kiwifruit calli and *N. benthamiana* leaves at 4 °C and 25 °C (Fig. 3D; Supplemental Figs. S6 and S12), respectively. These analyses imply that *AcePosF21* is not only involved in the cold-responsive pathway but also may play a role in regulating AsA synthesis.

Kiwifruit AcePosF21 regulates *AceGGP3* expression to increase AsA synthesis in response to cold stress

We sought to establish whether AcePosF21 was able to activate the expression of *AceGGP3* to regulate AsA synthesis. In

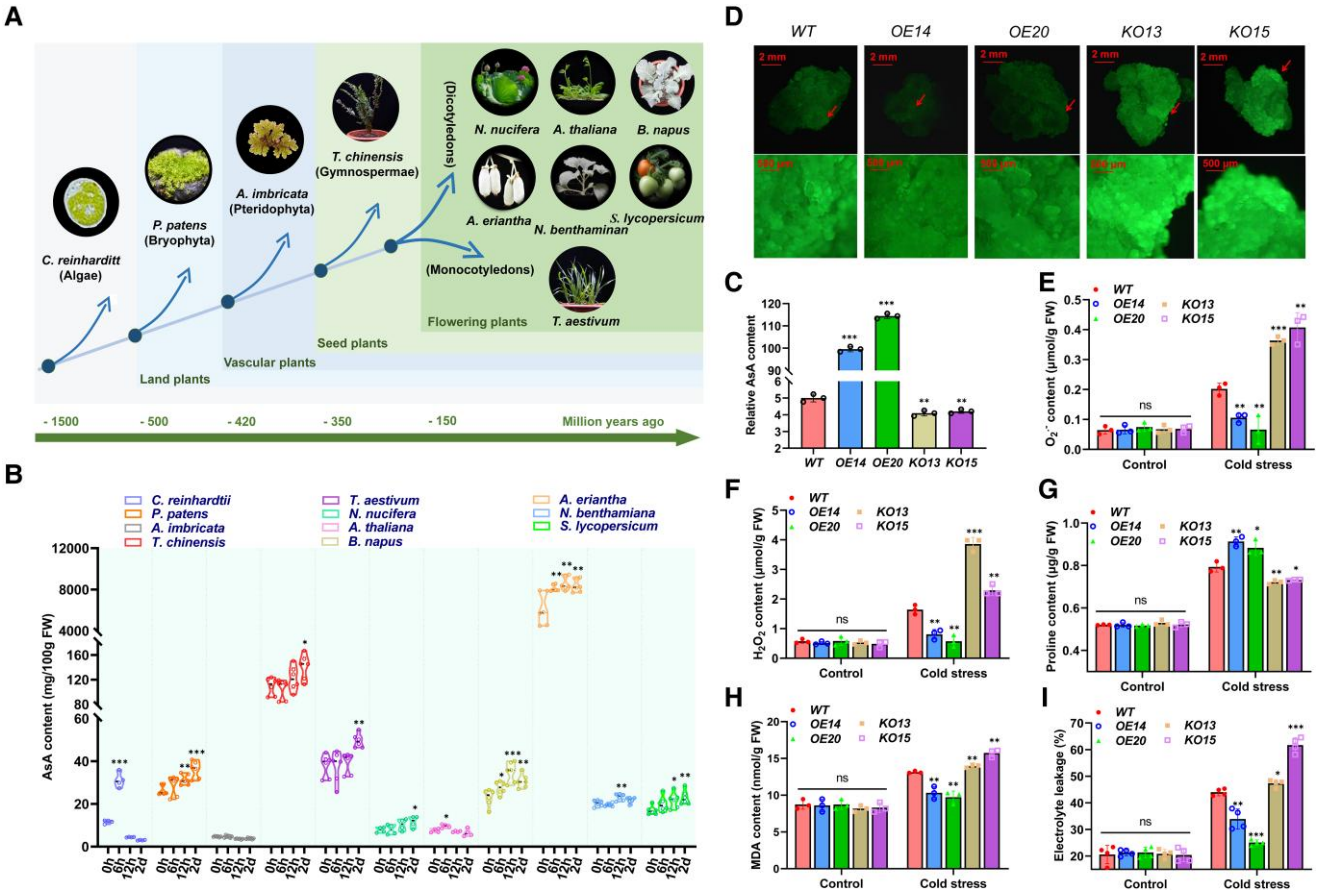

Figure 1. Ascorbic acid (AsA) and *AceGGP3* are induced by cold stress and alleviated ROS damage. **A)** The species being studied represent the major clades and subclades in the plant kingdom. **B)** AsA concentrations increased in most plants after exposure to cold (4 °C) for 0 h, 6 h, 12 h, and 2 d (n = 4–6). **C)** Relative AsA content of wild-type (WT), *AceGGP3*-overexpression (*OE14* and *OE20*), and *AceGGP3*-edited (*KO13* and *KO15*) lines of kiwifruit calli (AsA content of wild-type was taken as 5 for normalization). **D)** Under cold treatment (4 °C, 6 h), fewer fluoresce (ROS) were detected in *AceGGP3*-overexpression kiwifruit calli than that in *AceGGP3*-editing calli and WT. **E–I)** The content of $O_2^{\cdot-}$ **E)**, H_2O_2 **F)**, proline **G)**, MDA **H)**, and electrolyte leakage ($n = 4$) **I)** in WT, *AceGGP3* overexpression and editing calli after 25 °C (control) or 4 °C (cold stress) for 6 h. Error bars denote the standard deviation (± SD), $n = 3$ to 4. Significant differences were detected by *t*-test (*$P < 0.05$; **$P < 0.01$; ***$P < 0.001$).

the Y1H experiment, AcePosF21 (pB42AD::AcePosF21) could interact directly with *AceGGP3* promoter (*LacZ*::*AceGGP3pro*) to activate *AceGGP3* expression (Fig. 4A). This activating function was further confirmed using the Dual-LUC assay, showing an increased LUC/REN ratio in *N. benthamiana* leaves when co-infiltrated with both of *AceGGP3* promoter (*AceGGP3pro*::*LUC*) and *AcePosF21* expression construct (*35S*::*AcePosF21*) (Fig. 4B). Next, an EMSA assay was conducted in vitro and revealed that AcePosF21-His fusion proteins (Supplemental Fig. S13) could bind the DNA biotin-labeled probe (−1452 bp), which was weakened by the unlabeled competitor. Notably, the biotin-labeled mutant probe cannot bind to the AcePosF21-His fusion proteins (Fig. 4C). Finally, a ChIP-qPCR assay was performed using cell extracts from wild-type kiwifruit calli or transgenic calli expressing a FLAG—fuzed AcePosF21 protein under the 35S promoter. The fragment containing *AceGGP3* had higher enrichment in AcePosF21—FLAG transgenic rather than wild-type kiwifruit calli (Fig. 4D). Therefore, AcePosF21 binds *AceGGP3*'s promoter and activated its expression both in vitro and in vivo.

To verify *AcePosF21* positively regulates AsA accumulation in kiwifruit, transient overexpression, and silencing (VIGS) assays were implemented in calli of tissue culture explants and on-vine fruit. Transient-overexpress *AcePosF21* in the fruit and calli resulted in significantly higher *AceGGP3* expression and AsA content than the control, while transient antisense *AcePosF21* reduced *AceGGP3* transcripts and AsA content (Supplemental Fig. S4, E to G; Supplemental Fig. S14). Second, the link between *AcePosF21* and AsA accumulation in kiwifruit was unequivocally established using calli in which *AcePosF21* was overexpressed by 35S promoter and edited by CRISPR/Cas9 system. Three independent transgenic calli of *AcePosF21*-overexpression (*OE-AcePosF21#7*, *OE-AcePosF21#15*, and *OE-AcePosF21#20*) were obtained, which increase AsA content by 1.6 to 2.2-fold and enhance *AceGGP3* by 4.1 to 5.0-fold compared to WT (Supplemental Fig. S4, H to J). Two *AcePosF21*-edited lines (*posf21#9* and *posf21#27*) were generated with 1 and

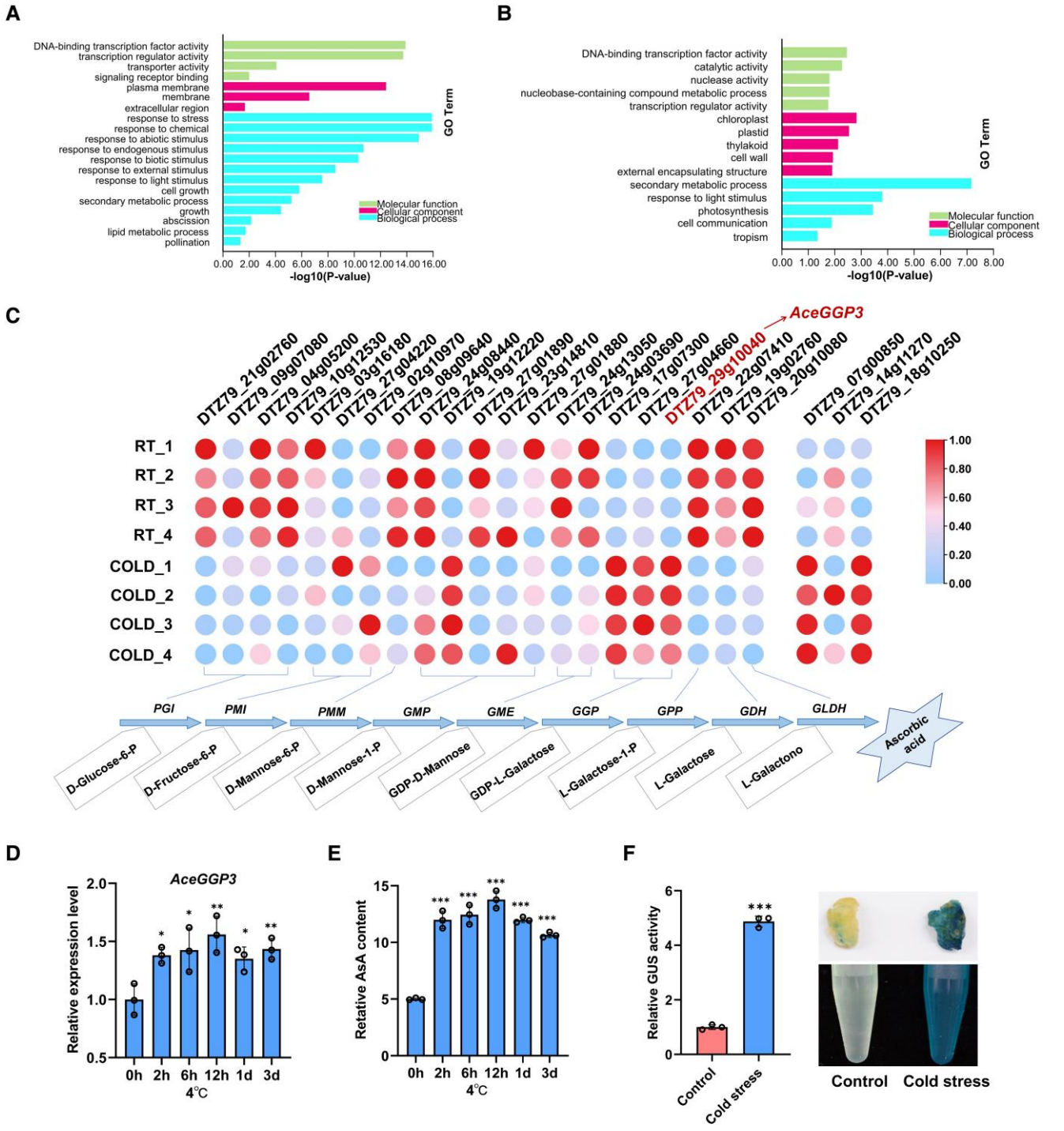

Figure 2. The *AceGGP3* expression is induced by cold stress. **A–B)** Gene ontology (GO) analysis of significantly up-regulated **A)** and down-regulated **B)** genes in kiwifruit calli at RT (room temperature) and COLD (4 °C) for 6 h. **C)** Expression profiles of 21 genes of L-galactose pathway and 3 transcription factors in kiwifruit under RT and COLD. Log-transformed expression values range from 0 to 1. **D)** RT-qPCR analysis of *AceGGP3* expression of kiwifruit (*A. eriantha*) calli treated at 4 °C for 0 h, 2 h, 6 h, 12 h, 1 d, and 3 d. **E)** Relative AsA content of kiwifruit calli in **D)**. AsA content of calli in 0 h was taken as 5 for normalization. **F)** Relative GUS activity and histochemical staining of the *AceGGP3* promoter expression construct *AceGGP3::GUS* in transgenic kiwifruit calli at 25 °C (control) and 4 °C (cold stress) for 9 h. Error bars denote the standard deviation (± SD), $n = 3$. Significant differences were detected by *t*-test (*$P < 0.05$; **$P < 0.01$; ***$P < 0.001$).

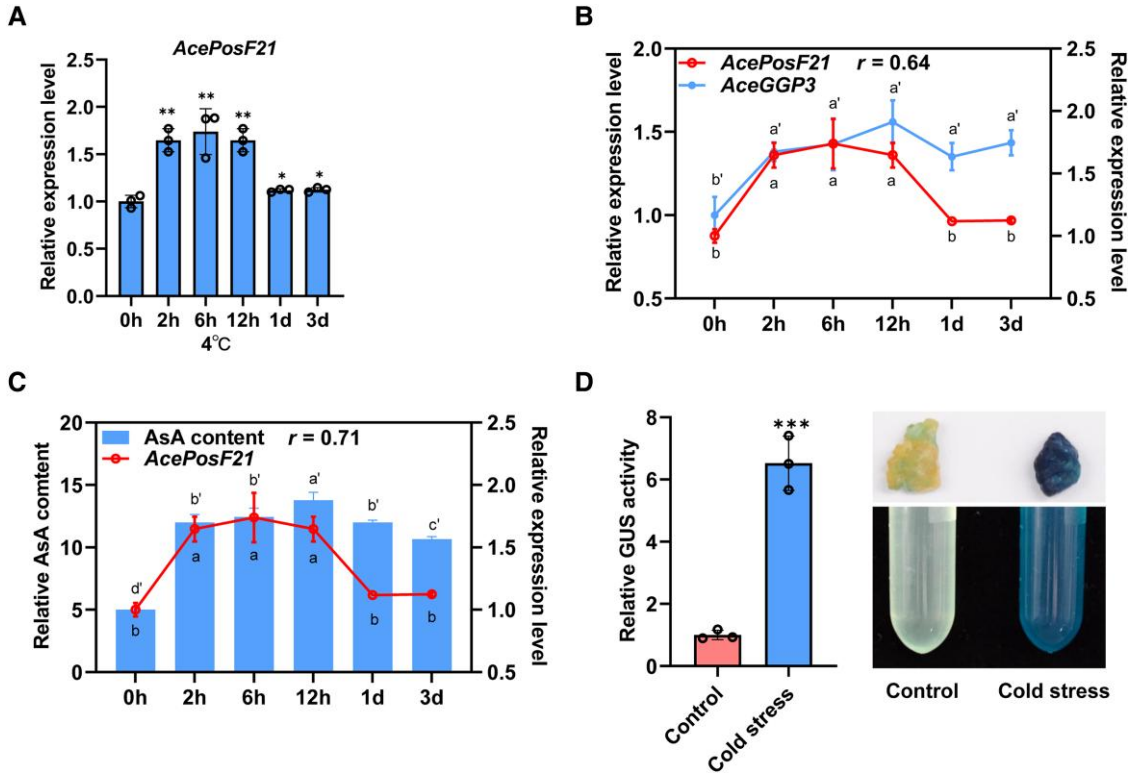

Figure 3. Identification and characterization of *AcePosF21*. **A)** RT-qPCR analysis of *AcePosF21* in kiwifruit calli after being treated at 4 °C for 0 h, 2 h, 6 h, 12 h, 1 d, and 3 d. **B–C)** Correlation between the expression of *AcePosF21* with *AceGGP3* **B)** and AsA content **C)** of kiwifruit calli after cold treatment. **D)** Relative GUS activity and histochemical staining of the *AcePosF21* promoter expression construct *AcePosF21::GUS* in transgenic kiwifruit calli at 25 °C (control) and 4 °C (cold stress) for 9 h. Error bars denote the standard deviation (± SD), $n = 3$. For **A)** and **D)**, significant differences were detected by *t*-test (*$P < 0.05$; **$P < 0.01$; ***$P < 0.001$). For **B)** and **C)**, different letters above and below the bars indicated significant differences ($P < 0.05$) as obtained by the one-way ANOVA test.

2 bp base deletion in the first exon, which caused premature termination of bZIP protein at positions corresponding to amino acids 209 and 262, respectively (Fig. 4, K to M; Supplemental Fig. S15). Consequently, the AsA concentration, expression of *AcePosF21* and *AceGGP3* declined by 42% to 49%, 25.7% to 26.6%, and 32.5% to 37.9% in comparison with WT, respectively (Fig. 4, N and O). Collectively, these results show that *AcePosF21* positively regulates AsA accumulation in kiwifruit.

AcePosF21 alleviated ROS damage during cold stress

To establish whether *AcePosF21* alleviated ROS during cold stress, kiwifruit WT and transgenic calli (overexpression and editing *AcePosF21*) were exposed to 25 °C and 4 °C for 6 h, after which they were sampled and evaluated for indicators of stress. The expression level of *AcePosF21* increased in all overexpression lines under cold stress (Fig. 5A). As observed previously, the calli overexpressing *AcePosF21* showed less ROS production than WT, whereas the content of ROS in the *AcePosF21*-edited lines evidently increased after cold treatment (Fig. 5B). Consistently, lighter staining of DAB and NBT (Supplemental Fig. S16A), $O_2^{\cdot-}$ and H_2O_2 contents were significantly lower in the calli overexpressing *AcePosF21* compared to WT, while they were 1.7 to 2.1 times higher in *AcePosF21*-edited lines at cold stress (Fig. 5, C and D). Compared with WT, both EL and MDA levels were lower in the calli overexpressing *AcePosF21*, but higher in *AcePosF21*-edited lines (Fig. 5, E and F), implying that cell injury was higher if *AcePosF21* was mutated. Overexpressing *AcePosF21* also increased proline, and editing of *AcePosF21* decreased proline content in transgenic calli (Fig. 5G). The fresh weight of *AcePosF21*-overexpressing calli is higher than that of *AcePosF21*-editing calli at low-temperatures (Supplemental Fig. S16B). In summary, these results clearly demonstrate that *AcePosF21* is able to reduce the negative effects of cold stress in kiwifruit. Combined with the ability to activate the expression of *AceGGP3* by direct binding to its promoter, we conclude that AcePosF21 acts as an important transcriptional regulator of AsA-mediated alleviated ROS damage by cold stress.

AcePosF21 interacts with AceMYB102 coordinately regulates AsA synthesis and alleviates ROS damage

Transcriptional activation often occurs through the cooperative binding of two or more TFs (Bemer et al. 2017). Here, an AcePosF21-DB bait was constructed to screen for candidate proteins from our yeast library, which might interact with AcePosF21 to synergistically regulate AsA synthesis. As a result, a protein DTZ79_18g10250 with homology to plant

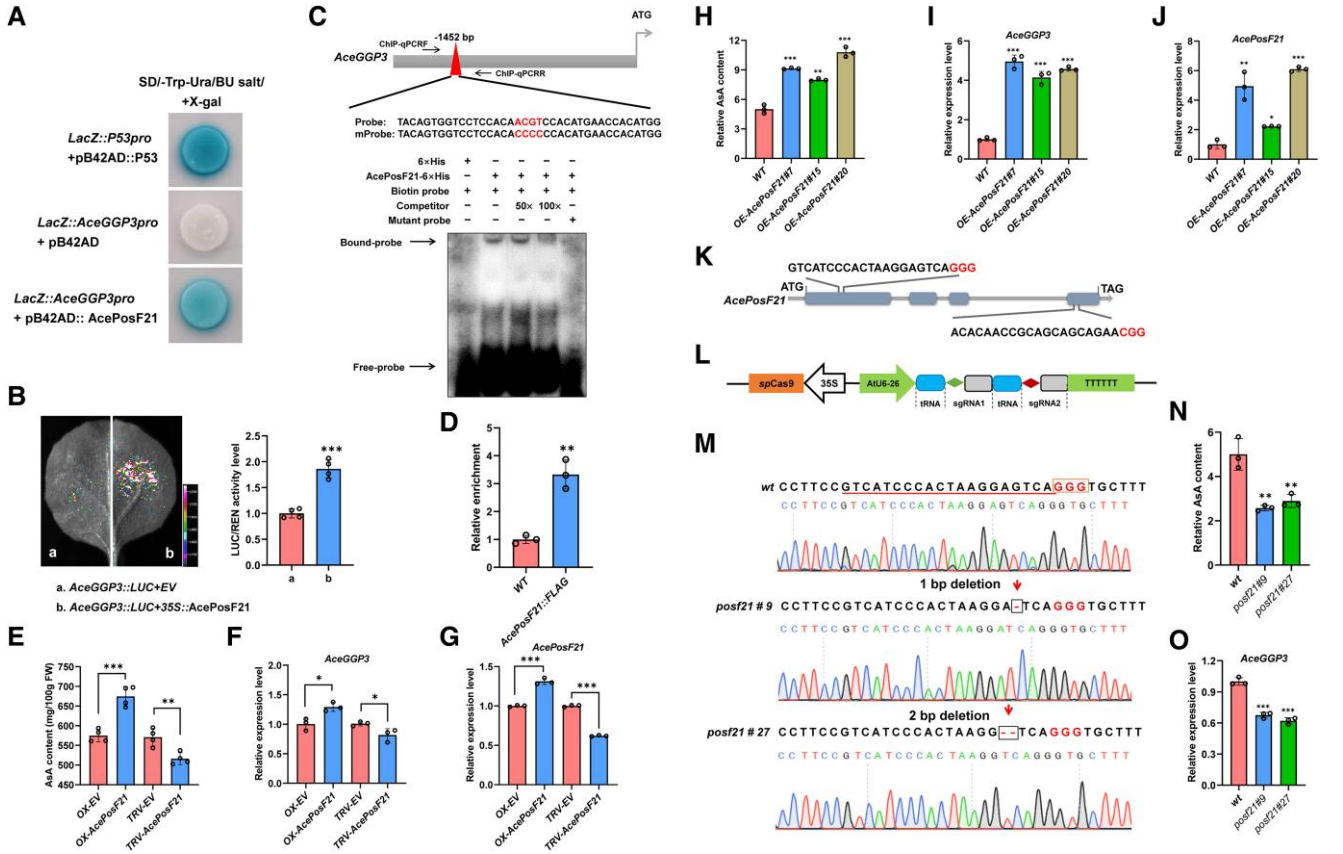

Figure 4. *AcePosF21* directly binds to the *AceGGP3* promoter and positively regulates AsA synthesis. **A)** Y1H assay showing the interaction between *AcePosF21* and *AceGGP3* promoter (*LacZ::AceGGP3pro*). The yeast strain was grown on SD/-Trp/-Ura/BU salt/X-gal media for 3 d. *LacZ::P53pro* + pB42AD::P53: positive control; *LacZ::AceGGP3pro* + pB42AD: negative control. **B)** Luciferase activity analysis shows that AcePosF21 activates the transcription of *AceGGP3* promoter based on the LUC/REN ratio (right) in *N. benthamiana* leaves. A representative photograph was shown (left picture), and LUC/REN ratio of empty vector control (EV) was taken as 1 for normalization ($n = 4$). **C)** The AcePosF21 binding on the promoter of *AceGGP3* (above) and electrophoretic mobility shift assay (EMSA) analysis of the AcePosF21 (below). The biotin-labeled probe 5′-TACAGTGGTCCTCCACAACGTCCACATGAACCACATGG-3′ was replaced with a biotin-labeled mutant probe 5′-TACAGTG GTCCTCCACACCCCCCACATGAACCACATGG-3′. The unlabeled wild-type probes were used as a competitor. 50 × and 100 × represent the rates as the competitor. The purified AcePosF21-6×His protein was incubated with the biotin-labeled probes, competitor, and mutant probes. The arrows indicated a bound DNA protein complex. +: presence; −: absence. **D)** Chromatin immunoprecipitation (ChIP) assay using *35S::AcePosF21-FLAG* transgenic kiwifruit calli. The Chromatin was immunoprecipitated with FLAG antibody, and quantitative real-time polymerase chain reaction (qPCR) was performed with the primers listed in Supplemental Table S3. Wild-type (WT) kiwifruit was used as control, and its value was set to 1. **E)** AsA content of kiwifruit fruits of *AcePosF21* transient expression at 7 d after vector infiltration (n = 4). OX-EV/TRV-EV: empty vector; *OX*: transient overexpression; *TRV*: transient antisense-expression. **F–G)** RT-qPCR analysis of *AceGGP3* **F)** and *AcePosF21* **G)** in **E)**. **H)** Relative AsA content (AsA content of WT was taken as 5 for normalization) of three *AcePosF21*-overexpression transgenic lines in kiwifruit calli. *OE*: stable overexpression of kiwifruit calli. **I–J)** RT-qPCR analysis of *AceGGP3* **I)** and *AcePosF21* **J)** expression in **H)**. **K)** A schematic map of the targeting sites in the exon regions (rectangle) of *AcePosF21*; the PAM motifs (NGG) are shown in the last three bases. **L)** Schematic diagram of the CRISPR/Cas9 vector and *AcePosF21* targeting sites (diamonds) within the tRNA-sgRNA fusions. **M)** Sequences and chromatograms of *AcePosF21* in WT and two independent homozygous mutant calli (*posf21#9* and *posf21#27*). The target sequence is underlined, the PAM sequence is contained in the rectangle after the target sequence, and the dashes indicate deletions. **N)** Relative AsA content of *AcePosF21*-editing lines. **O)** RT-qPCR analysis of *AceGGP3* in **N)**. Error bars denote the standard deviation (±SD), $n = 3$ to 4. Significant differences were analysis by *t*-test using GraphPad Prism 8 (*$P < 0.05$; **$P < 0.01$; ***$P < 0.001$).

R2R3-MYB family TF MYB102 was discovered and we annotated it as AceMYB102 (Supplemental Fig. S17). Y2H domain mapping exhibited that the N-terminal half (AcePosF21^{N}, 1–750 aa) of AcePosF21 interacted with AcebMYB102 (Fig. 6, A and B). Subsequently, two transient expression assays were applied to verify that AcePosF21 interacted with AcebMYB102 in vivo. The luciferase complementation assay demonstrated that only when AcePosF21-nLUC and AceMYB102-cLUC were infiltrated into *N. benthamiana* leaves could a fluorescent signal be detected (Fig. 6, C and D). In the BiFC assay, AcePosF21-NYFP, and AceMYB102-cYFP were co-transformed into onion epidermal cells, and

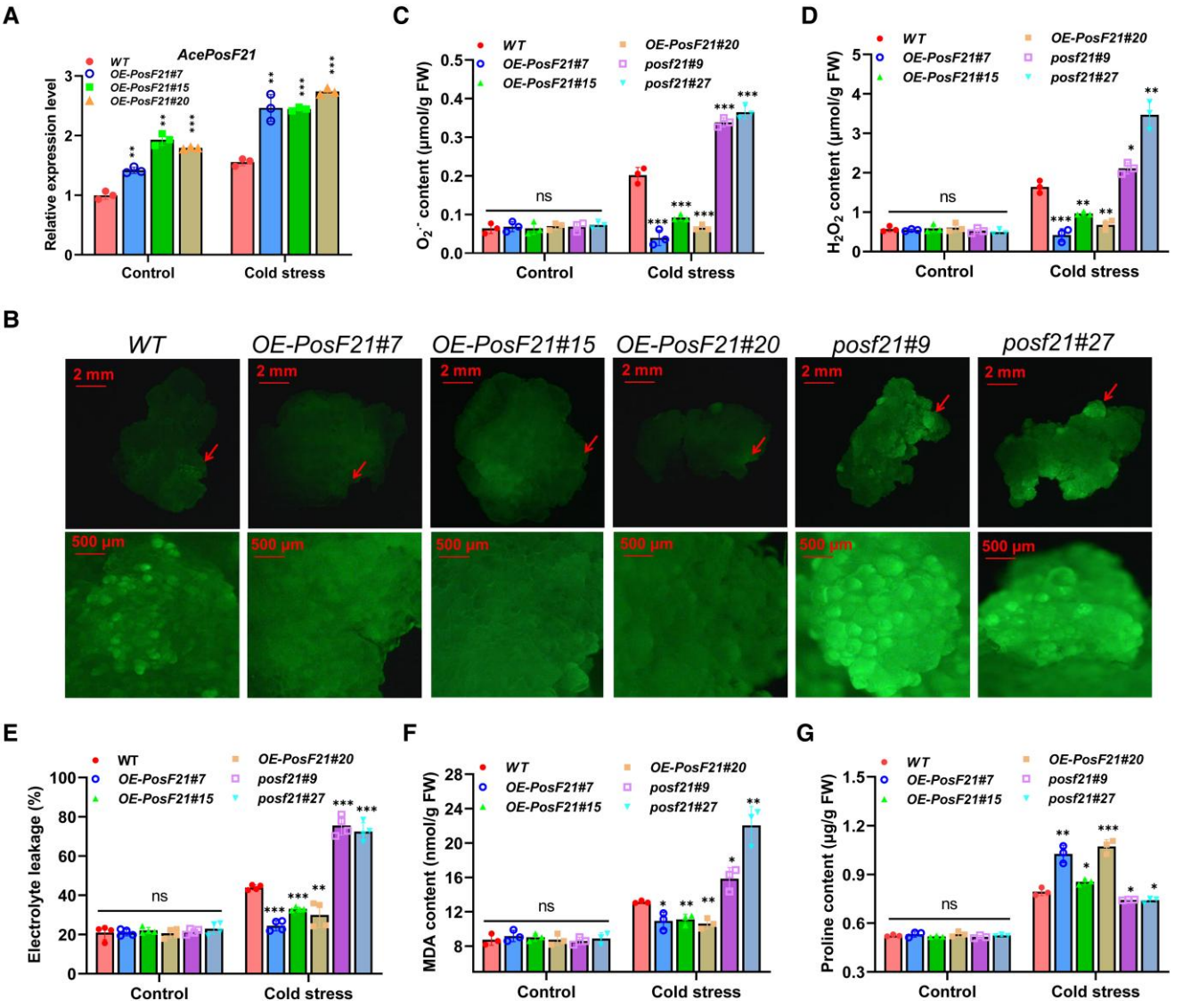

Figure 5. *AcePosF21* positively alleviates ROS damage by cold stress in kiwifruit. **A)** The expression level of *AcePosF21* in WT and transgenic calli of *AcePosF21*-overexpression lines under 25 °C (control) or 4 °C (cold stress) for 6 h. **B)** The variation of fluorescence intensity showed the difference in ROS content among WT, *AcePosF21*-overexpression, and mutant calli of kiwifruit after cold treatment (4 °C) for 6 h. **C–G)** The content of $O_2^{\cdot-}$ **C)**, H_2O_2 **D)**, electrolyte leakage **E)**, MDA **F)** and proline **G)** of wild-type, *AcePosF21*-overexpression, and mutant calli under 25 °C (control) or 4 °C (cold stress) for 6 h. Error bars indicate ± SD in the above experiments ($n = 3$ to 4). Significant differences were detected by *t*-test (*$P < 0.05$; **$P < 0.01$; ***$P < 0.001$).

fluorescence signals indicated AcePosF21 physically interacts with AceMYB102 in the cell nucleus (Fig. 6, E and F). Moreover, a pull-down assay was performed where the AceMYB102-glutathione S-transferase (GST) fusion protein was precipitated as a protein complex with AcePosF21-6×His purified protein rather than 6×His alone by GST resin, indicating AcePosF21 physically interacts with AceMYB102 in vitro (Fig. 6G; Supplemental Fig. S13). To sum up, AcePosF21 interacts with AceMYB102 and co-expressed in vitro and in vivo.

The subcellular localization assay revealed that AceMYB102 was located in the nucleus (Supplemental Fig. S18) and had transcriptional activation activity in yeast cells (Supplemental Fig. S19), indicating that AceMYB102 was able to act as a TF and coordinately regulate AsA synthesis with AcePosF21. The Dual-LUC assay was performed to determine whether AceMYB102 contributes to AsA synthesis. In *N. benthamiana* leaves, expression of both *AcePosF21* (*35S::AcePosF21*) and *AceMYB102* (*35S::AceMYB102*) induced a higher accumulation of *AceGGP3* transcript than *AcePosF21* alone (3.1- and 1.9-fold compared to empty vector control, respectively) (Fig. 6H). In kiwifruit, AsA content and *AceGGP3* expression in fruits and calli increased significantly when *AcePosF21* and *AceMYB102* were co-injected compared

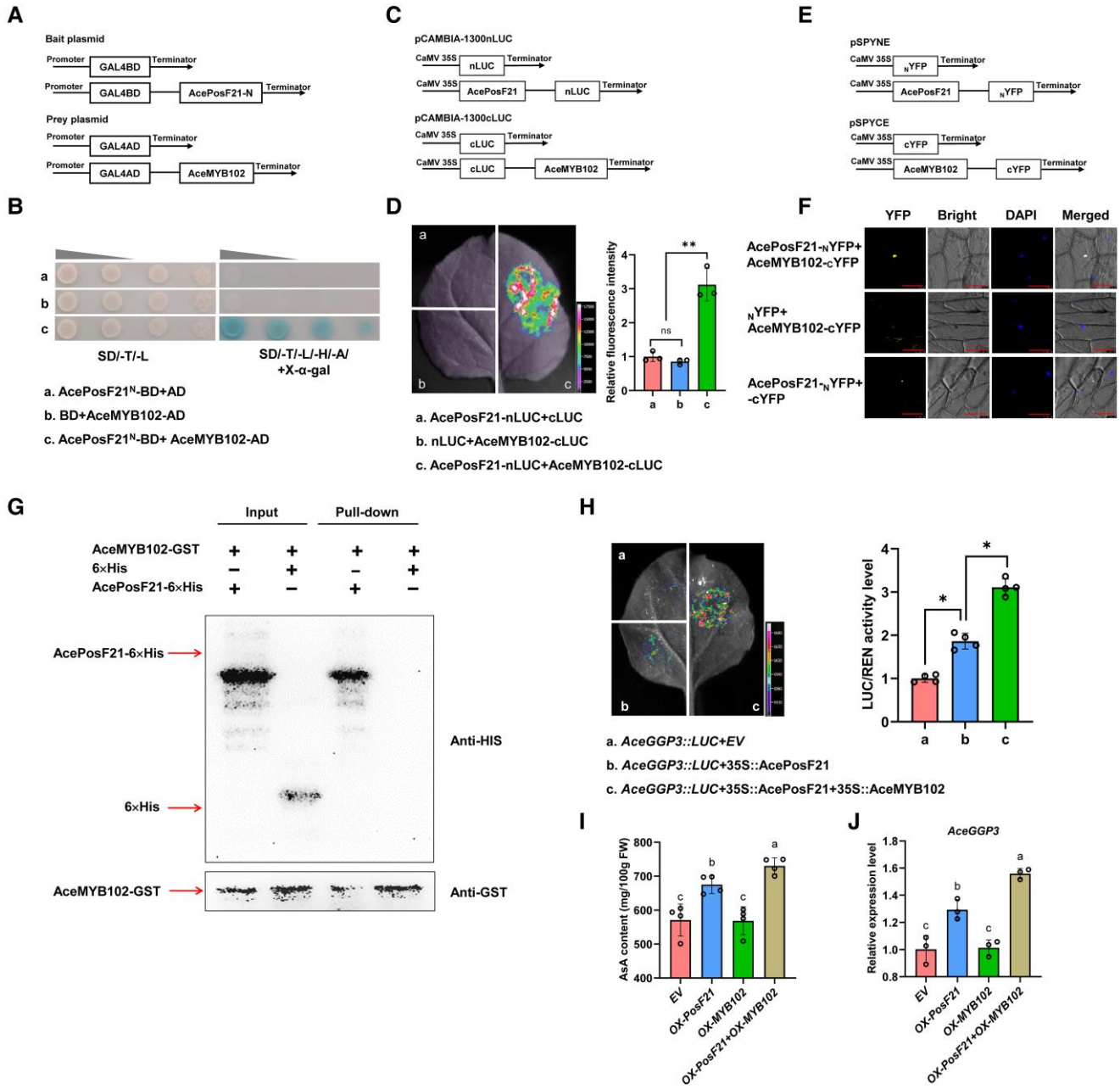

Figure 6. AcePosF21 interacts with AceMYB102 which coordinately upregulates AsA synthesis. **A)** Conventional diagram of yeast two-hybrid assay. The N-terminus of *AcePosF21* CDS was fuzed with the activation domain of pGBKT7 (BD) to generate AcePosF21^{N}-BD as the bait, AceMYB102-AD as the prey. **B)** Y2H assay indicates that AceMYB102 interacts with AcePosF21 in yeast in vivo. The transformed yeast strains were grown at 30 °C for 3 d. Empty vector (AD and BD) as a control. **C)** Schematic map of luciferase complementation assay. The CDS of *AcePosF21* and *AceMYB102* were fuzed with the N-terminus and C-terminus of the luciferase protein (LUC) in pCAMBIA1300-nLUC and pCAMBIA1300-cLUC vector, respectively. **D)** Luciferase complementation assay demonstrates AceMYB102 interacted with AcePosF21 in *N. benthamiana* leaves. **E)** Diagrammatic drawing of bimolecular fluorescence complementation (BiFC) assay. The CDS of *AcePosF21* and *AceMYB102* were fuzed with the N-terminus and C-terminus of the yellow fluorescent protein (YFP) in pSPYNE-35S and pSPYCE-35S vector, respectively. **F)** BiFC assay infers the interaction between AcePosF21 and AceMYB102 in the onion epidermal cells. The empty vector ($_{N}$YFP and $_{C}$YFP) was used as the control. Scale bars = 100 μm. **G)** An in vitro pull-down assay verified the interaction between AcePosF21 and AceMYB102. AceMYB102-GST protein was incubated with immobilized AcePosF21-6×His or 6×His protein, and immune-precipitated fractions were detected by Anti-GST antibody. **H)** Dual-LUC assay showed that the transcription of *AceGGP3* was activated by AcePosF21 and AceMYB102 individually or collectively ($n = 4$). **I)** AsA content of *AcePosF21* and *AceMYB102* co-expression in fruits. EV: empty vector; *OX:* transient overexpression; *OX + OX*: transient co-overexpression; $n = 4$. **J)** RT-qPCR analysis of *AceGGP3* in the plants in **I)**. All error bars denote standard deviation (±SD), $n = 3$ to 4. For H, significant differences were detected by *t*-test (*$P <$ 0.05; **$P < 0.01$; ns: no significance). For **I)** and **J)**, different letters above the bars indicated significant differences ($P < 0.05$) as obtained by the one-way ANOVA test.

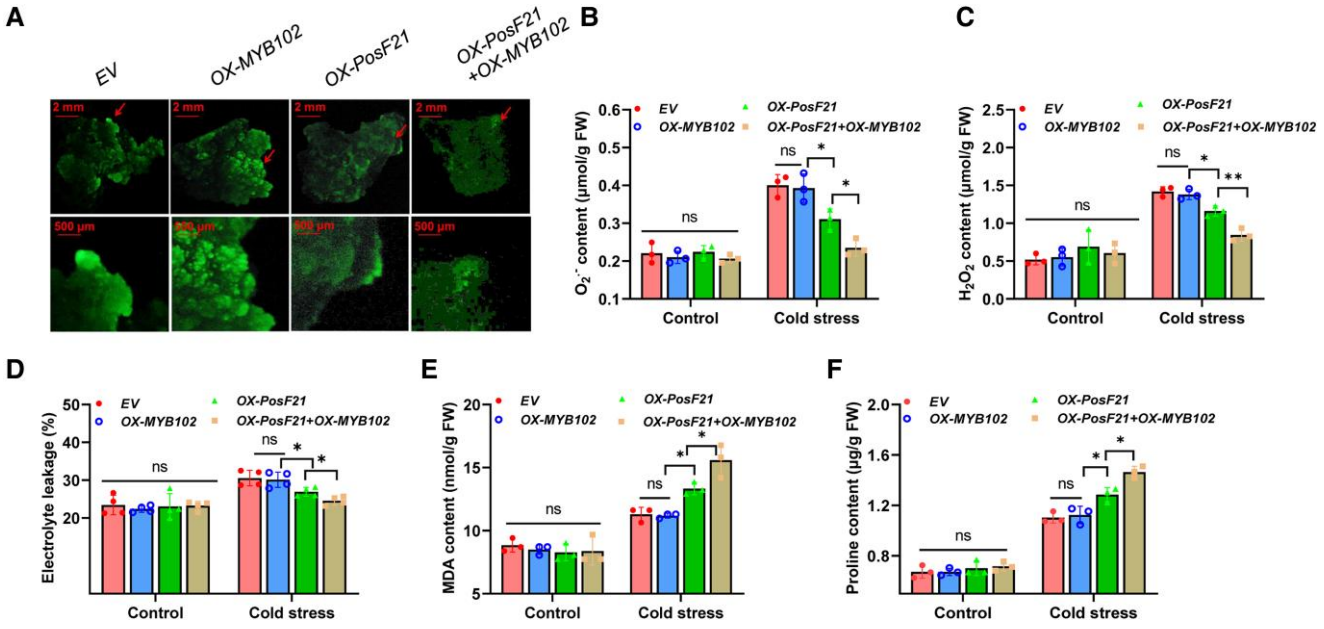

Figure 7. AcePosF21 interacts with AceMYB102 to alleviate ROS damage from cold stress. **A)** The variation of fluorescence intensity showed the difference in ROS content among transient expression in kiwifruit calli after 25 °C (control) or 4 °C (cold stress) for 6 h. EV: empty vector; *OX*: transient overexpression; *OX* + *OX*: transient co-overexpression. **B–F)** The content of $O_2^{\cdot-}$ **B)**, H_2O_2 **C)**, electrolyte leakage **D)**, MDA **E)** and proline **F)** of the calli in **A)**. Error bars indicate ± SD in the above experiments, $n = 3$ to 4. Significant differences were detected by *t*-test (*$P < 0.05$; **$P < 0.01$).

to only overexpressed *AcePosF21*. A lesser increase in AsA content and *AceGGP3* expression was detected with *AcePosF21* and they barely changed when *AceMYB102* was overexpressed alone (Fig. 6, I and J; Supplemental Fig. S20), indicating that AceMYB102 interacts with AcePosF21 to coordinately promote AsA synthesis.

AceMYB102 expression was induced by cold stress in both calli and fruit of kiwifruit (Fig. 2C and Supplemental Fig. S21). To determine whether *AceMYB102* decreased cold damage in kiwifruit, physiological indexes were systematically determined for transient expression plants. The overexpression of *AceMYB102* alone did not substantially reduce ROS fluorescence intensity unless co-expressed with *AcePosF21* (Fig. 7A), suggesting that AceMYB102 and AcePosF21 coordinately regulated AsA synthesis and prevented ROS damage. Compared to empty vector or calli only overexpressed *AceMYB102*, co-expressing *AceMYB102* and *AcePosF21* also resulted in lighter staining of DAB and NBT (Supplemental Fig. S22), decreased $O_2^{\cdot-}$ and H_2O_2 contents in the calli (Fig. 7, B, C). Consistently, both EL and MDA content were lower, and proline levels were higher in calli of *AceMYB102* and *AcePosF21* co-expression, whereas no significant difference between EV and *AceMYB102*-overexpression calli (Fig. 7, D to F). These data showed that *AcePosF21* and *AcePosF21* plus *AceMYB102* but not *AceMYB102* alone could mitigate plant cold injury.

Discussion

Cold is one of the most vital abiotic stresses restricting plant growth, development, geographical distribution, and yield (Rivero et al. 2001; Suzuki and Mittler 2006; Xiao et al. 2018). Cold stress triggers ROS production and stimulates lipid peroxidation, leading to cell membrane damage and promoting cell death (Ruelland et al. 2009). Increasing evidence indicates that antioxidant capacity is positively associated with cold tolerance (Sun et al. 2019). AsA is a potent antioxidant molecule (Noctor and Foyer 1998), which plays a crucial role in quenching intermediate/excited reactive forms of molecular oxygen either directly or through enzymatic catalysis (Ye et al. 2012). Here, the accumulation of AsA under cold stress was shown to be a common phenomenon in plants, from *Chlamydomonas*, a single-celled green alga, to angiosperms, such as wheat, tomato, and kiwifruit (Fig. 1). Interestingly, we identified a PosF21 transcription factor, which could mediate-AsA synthesis and reduce oxidative damage caused by cold stress (Figs. 3 to 5).

Cold-induced AsA is a positive factor to reduce cold damage

In line with the main enzymatic antioxidants (such as superoxide dismutase, catalase, glutathione peroxidase), the nonenzymes such as AsA and GSH are among the major nonenzymatic antioxidants against damage of ROS inducing by kinds of environmental stresses (Conklin et al. 1996; Sanmartin et al. 2003; Pavet et al. 2005). Cold stress is environmental stress known to induce oxidative damage in plants. Low-temperature-mediated increase in superoxide (O^{-2}) has been observed earlier in the leaves of a number of plants, including cucumber, maize, and millet (Lukatkin 2002). If not

metabolized, ROS can initiate damage to cellular membranes by oxidizing membrane biomolecules such as lipids and proteins (Anjum et al. 2014; Cao et al. 2022). The AsA-mediated antioxidant defense metabolism against abiotic stress was reported in different plants, such as canola (*Brassica napus*) and barley (*Hordeum vulgare*) under salinity (Bybordi 2012; Raza et al. 2013; Agami 2014), and canola under drought (Shafiq et al. 2014), to name a few. Thus, AsA plays an important role in scavenging ROS from plants to counteract the damage caused by stressful environments. However, whether plants spontaneously synthesize ascorbic acid in response to cold stress is not well characterized. Except for *Azolla imbricata*, endogenous ascorbic acid content of 10 plants in this study was significantly elevated than that of the untreated samples (Fig. 1B). Although differences exist in how fast and intense this accumulation of different plants, this may be related to the speed with which different plants respond to cold. Using kiwifruit materials with different AsA concentrations created by transgenic and gene-editing, we further proved that the transgenic plants with higher AsA concentrations accumulated less ROS than the WT (Fig. 1, D to I). Therefore, higher AsA content endogenously rather than fed could reduce membrane damage and ROS accumulation in plants under cold stress.

Cold stress-induced *AcePosF21* expression reduces kiwifruit oxidative damage via promoting the AsA biosynthesis

The bZIP transcription factor was one of the key TFs involved in plant perception and adaptation to the various extreme environment, e.g. drought, salinity, heat, oxidative, and cold stress (Xiang et al. 2008; Lu et al. 2009; Hwang et al. 2014; Xiao et al. 2018; Agarwal et al. 2019). Until now, there are still few plant bZIPs acting as critical components for the orchestration of cold response, such as rice (Liu et al. 2018a, 2018b; Liu et al. 2019), *Brassica rapa* (Hwang et al. 2014), *A. thaliana* (An et al. 2018a), radish and banana (Ito et al. 1999; Shekhawat and Ganapathi 2014). In this study, a bZIP TF in kiwifruit, namely *AcePosF21*, was identified and defined as a positive regulator for cold stress. The overexpression of the *AcePosF21* significantly promoted *AceGGP3* expression which in turn increased AsA accumulation and removed excess ROS (Figs. 3 to 5). Previous studies indicated that plant cells have evolved a complex homeostasis system to produce protective compounds, e.g. maltose (Peng et al. 2014), starch (Liu et al. 2020, 2021), and sucrose (Dahro et al. 2022), for lessening the negative effects of cold stress. Here, we found a regulatory mechanism, *AcePosF21* mediates *AceGGP3* expressed, which produced a stronger antioxidant (ascorbic acid) to protect the plant cell homeostasis during the early stages of cold stress (Figs. 4 and 5). However, the effectiveness and mechanism of maltose, starch, sucrose, and L-ascorbic acid in enhancing the cold resistance of different plants remain to be explored.

Emerging evidence infers that bZIPs can form a protein complex with MYBs to modulate the synthesis and metabolism of compounds in plants (Hassani et al. 2020). For example, MdbZIP44 promotes anthocyanin synthesis by interacting with MdMYB1 to enhance the binding to downstream target gene promoters (An et al. 2018b). Here, we found that the R2R3-MYB, AceMYB102 interacted with AcePosF21 using Y2H, BiFC, Luciferase complementation, and pull-down assays (Fig. 6, A to G). It is noteworthy that AceMYB102 was not found to bind directly to the *AceGGP3* promoter and so does not independently regulate AsA synthesis in kiwifruit, but can further activate *AceGGP3* transcription by forming a protein complex in concert with AcePosF21 resulting in additively enhanced AsA accumulation and reduce oxidative damage (Figure 6, H and I; Fig. 7; Supplemental Fig. S20).

Altering AsA synthesis to improve plant abiotic stress tolerance

Currently, improving abiotic stress tolerance is a key strategy for modern agricultural breeding. Genetically engineered crop plants have been constantly generated, particularly with higher abiotic stress such as superior drought and salinity tolerance. Potentially, AsA can improve plant yield and growth as a potential regulator of different mechanisms under adverse factors, so over-accumulation of AsA in plants through gene (s) engineering could efficiently increase plant stress tolerance (Macknight et al. 2017). To improve tolerance to abiotic stresses, overexpression of the enzymes involved in the biosynthesis of AsA can be targeted to regulate AsA contents of plants. In the past, such efforts have paid off on many crops. For example, overexpression of *FaGalUR* increased the AsA concentration of tomato fruits and leaves, improving plant tolerance to low-temperatures (Cai et al. 2015). Similarly, overexpression of *MfAIR12* in *Arabidopsis* increases the AsA concentration, as well as the expression of *CBF* and its downstream cold-responsive, resulting in higher cold tolerance (Wang et al. 2021). In contrast, the *air12* or *KOS1* mutant had reduced AsA content and decreased cold tolerance in *Arabidopsis* (Wang et al. 2021). Moreover, overexpression of *SlGMEs* was reported to cause AsA accumulation with enhanced cold tolerance in tomatoes (Zhang et al. 2011). Here, overexpressing of *AceGGP3* indeed improved cold tolerance in kiwifruit calli, whereas knockout of *AceGGP3* and subsequent lower AsA had increased susceptibility to cold stress (Fig. 1). The recent finding that increases in AsA can result in increased ABA levels (Bulley et al. 2021) suggests a possible hierarchy in response to a cold stress event. Starting with cold stress, the stress is sensed and followed by an increase in ROS, then the response to ROS is to elevate AsA through *AcePosF21* and in some cases together with *AceMYB102*. Thus, there may be switching on of AsA synthesis and ROS-related responses mediated through *AcePosF21*.

In conclusion, our findings demonstrate that AcePosF21 mediates the *AceGGP3*-AsA synthesis in kiwifruit and acts

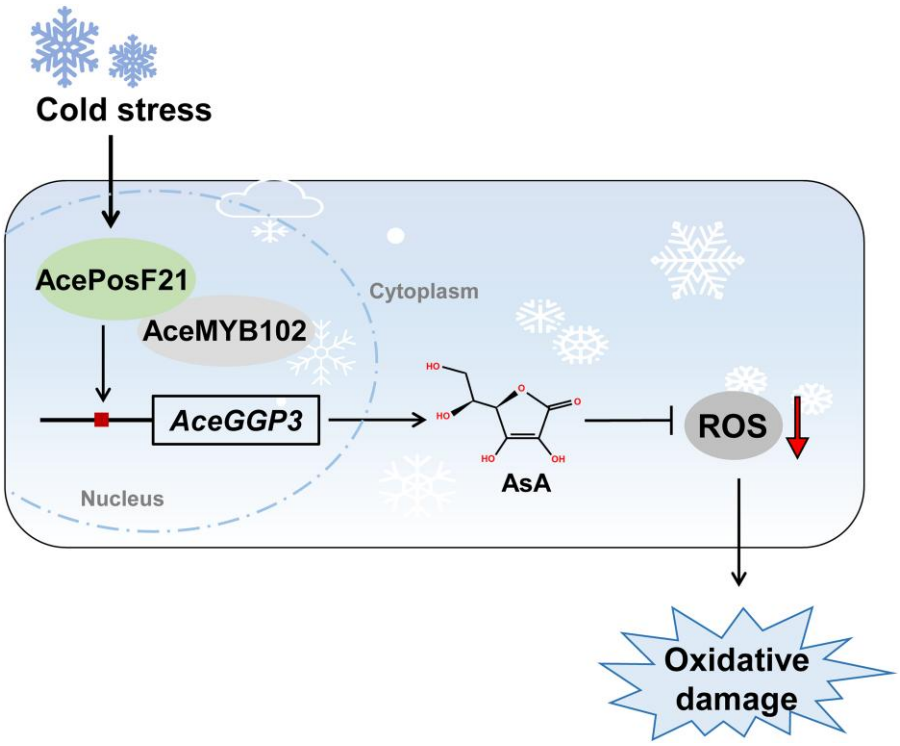

Figure 8. A proposed model for the regulatory mechanism of AcePosF21-mediated AsA biosynthesis and cold stress response. Under cold stress, *AcePosF21* is induced by the cold signal and then interacts with AceMYB102 to activate *AceGGP3* expression for upgrading the AsA synthesis to scavenge ROS, reducing the oxidative damage from cold stress in kiwifruit. AsA is induced by cold stress to eliminate excess ROS and reduce plant cold damage.

as a positive regulatory in cold stress. A working model was proposed to explain how AcePosF21 functions to alleviate ROS damage caused by cold stress (Fig. 8). The study provides valuable clues for creating genetic resources harboring higher AsA concentration and stronger cold resistance.

Materials and methods

Plant materials and cold stress treatments

The plant materials representing algae, bryophytes, ferns, gymnosperms, and angiosperms, namely, *C. reinhardtii*, *P. patens*, *A. imbricata*, *T. chinensis*, *T. aestivum* (wheat), *N. nucifera*, *A. thaliana*, *B. napus*, *A. eriantha* (kiwifruit), *N. benthamiana*, and *S. lycopersicum* (tomato) were cultivated in Wuhan Botanical Garden, Chinese Academy of Sciences (WBG) under natural conditions. Tomato, *N. benthamiana*, kiwifruit, *Arabidopsis*, winter rape, wheat, and *T. chinensis* were planted in the greenhouse, whereas *N. nucifera* and *A. imbricata* were grown in water with water-soluble fertilizer. *C. reinhardtii* was grown in a nutrient solution supplied with carbon dioxide for one week (Melero-Jiménez et al. 2022), and *P. patens* was grown under sterile conditions in a nutrient substrate for 2 months (Liu et al. 2014). The plants were selected for cold stress testing before flowering, except for kiwifruit at 80 d after flowering (DAF) and tomato at 45 DAF, respectively. For the cold stress treatments, they were exposed to 4 °C in the artificial climate chamber (300 lux, white light) and samples were collected at 0 h, 6, 12 h, and 2 d, except for kiwifruit, collected at 0 h, 2 h, 6 h, 12 h, 1 d, and 3 d. Algae cultures, plant leaf tissue, clumps (*P. patens*), or fruit samples (kiwifruit and tomato) were collected for each point of the experiment and subjected to AsA analysis. The molecular assays of kiwifruit and *N. benthamiana* were carried out in laboratories and greenhouses of WBG. Tissue-cultured materials for both *N. benthamiana* and kiwifruit were grown at 23–25 °C under long-day conditions (16 h : 8 h, light : dark photoperiod). Samples collected from individual plants were considered biological replicates (4 to 6 biological replicates) and were immediately frozen in liquid nitrogen and stored at −80 °C for later analyses.

Measurements of AsA content by HPLC

Total AsA content was measured by HPLC as described previously (Liu et al. 2022). The fruit and calli of kiwifruit were fully ground and extracted with 0.1% (w/v) metaphosphoric acid. After pretreatment and filtration, AsA concentration was determined in an Accela 1250 HPLC system (Thermo Fisher Scientific, USA) using a monomeric C18 column (WONDASIL C18, COLUMNS 5 μm, 4.6 × 150 mm, GL Sciences Inc., China) with 0.1% (w/v) metaphosphoric acid and acetonitrile (98:2, v/v) as the mobile phase. The flow

rate was 0.3 mL/min except for kiwifruit, for which 0.5 mL/min was chosen, and the injection volume of 10 μL was used.

RNA-seq, transcriptome analysis, cluster analysis, and tree construction

The Illumina RNA-seq, transcriptome analysis, cluster analysis, and tree construction of *A. eriantha* calli which was grown at 25 °C (named RT, room temperature) and exposed to 4 °C for 6 h (named COLD) were performed as previously described (Liu et al. 2022), and the filtered clean reads were mapped to the *A. eriantha* cv. White reference genome (Tang et al. 2019) by Hisat2 (DOI: 10.1038/s41587-019-0201-4). Kiwifruit and other species sequences were acquired from the kiwifruit database (http://kiwifruitgenome.org/) and the NCBI GenBank database (Supplemental Table S2).

RNA extraction and RT-qPCR analysis

Total RNA was isolated from the fruits and leaves using an RNA Extraction Kit (Magen, Guangzhou, China), and the cDNA was synthesized using a one-step gDNA removal and cDNA Synthesis SuperMix Kit (TransGen, Beijing, China). Reverse transcription quantitative PCR (RT-qPCR) was performed as described (Wang et al. 2018) using a *TransStart* Green qPCR SuperMix kit (TransGen, Beijing, China). The relative expression of each gene was determined using the $2^{-\Delta\Delta Ct}$ method and three biological replicates were used for all RT-qPCR analyses. The primers used in RT-qPCR are listed in Supplemental Table S3.

Construction of overexpression and gene-editing vectors and generation of transgenic kiwifruit lines

The full-length *AcePosF21* and *AceMYB102* CDS sequences were amplified from the cDNA of kiwifruit leaves and then inserted as *BamHI* fragments into the POE-3flag-DN vector containing the G418 and kanamycin resistance markers, placing them under the control of the 35S promoter to obtain *35::AcePosF21* and *35::AceMYB102* using a Basic Seamless Cloning and Assembly Kit (TransGen, Beijing, Chian), respectively. The *AcePosF21* was edited by CRISPR/Cas9 system as described previously (Wang et al. 2018; Liu et al. 2022). We selected specific sgRNA of *AcePosF21* using a CRISPR RGEN Tools (http://www.rgenome.net/?tdsourcetag=s_pcqq_aiomsg) and cloned it as *BsaI* fragments into CRISPR/Cas9 vector (pPTG-gRNA-Cas9-U6-26) to generate Cas9—AcePosF21. The recombinant plasmids were transformed into kiwifruit calli using *Agrobacterium tumefaciens* EHA105 (Wang et al. 2018). The primers used for overexpression and gene-editing constructs are listed in Supplemental Table S3.

Virus-induced gene silencing (VIGS) and transient transformation of kiwifruit calli and fruits

VIGS was performed as previously described (Liu et al. 2018a, 2018b; Yu et al. 2019) to silence the expression of *AcePosF21* and *AceMYB102*. The 400 bp fragments of CDS (Primers in Supplemental Table S3) were cloned from *AcePosF21* and *AceMYB102* and then inserted as *EcoRI/BamHI* fragments into the TRV2 vector to obtain *TRV-AcePosF21* and *TRV-AceMYB102*, respectively. For the transformation assay, *A. tumefaciens* EHA105 containing TRV1 + *TRV-AcePosF21*, TRV1 + *TRV-AceMYB102*, *35::AcePosF21* and *35::AceMYB102* were injected into fruits or transiently transformed calli of kiwifruit, respectively. Six days after infection, fruits, and calli were collected for RT-qPCR to screen putative VIGS samples which were used for further analysis.

Transcriptional activity analysis

The full-length CDS of *AcePosF21* and *AceMYB102* were PCR amplified and cloned as *BamHI/EcoRI* fragments into the pGBKT7 vector to obtain AcePosF21-DB and AceMYB102-BD and introduced into the AH109 yeast strain. The transcriptional activity analysis of AcePosF21-DB and AceMYB102-BD was performed according to the previously described method (Geng and Liu 2018).

Yeast one-hybrid (Y1H)

Y1H assay using the EGY48 Y1H system was performed as previously described (Huang et al. 2021). Briefly, the full-length CDS of *AcePosF21*, then cloned as *EcoRI/XhoI* fragments into pB42AD vector to generate the prey vector (pB42AD::AcePosF21) using a Basic Seamless Cloning and Assembly Kit (TransGen, Beijing, China), while the promoter of *AceGGP3* (2.6-kb) was fuzed as *KpnI/HindIII* fragments to the pLacZi vector to construct the baits (*LacZ::AceGGP3pro*). The *NcoI*-cut baits and prey vector were co-transformed into the yeast strain EGY48 using a high-efficiency yeast transformation method (Gietz and Schiestl 2007). The selection of the positively co-transformed cells was performed on SD/-Trp/-Ura medium and growing at 30 °C for 3 d. The resultant transformations were tested in an SD/-Trp/-Ura medium with β-galactosidase activity (SD/-Trp/-Ura/BU salt/X-gal) (Liu et al. 2022), with *LacZ::P53pro* + pB42AD::P53 as a positive control. The primers used in the Y1H assay were listed in Supplemental Table S3.

Yeast two-hybrid (Y2H) assays

For Matchmaker Gold Y2H Library Screening System, the *AcePosF21* CDS fragment encoding the N-terminus (1–750 amino acids, aa) was fuzed as *EcoRI/BamHI* fragments to a binding domain (BD) in the pGBKT7 vector to obtain the bait vector ($AcePosF21^{N}$-BD) using a Basic Seamless Cloning and Assembly Kit (TransGen, Beijing, China) and introduced into Y2H gold yeast strain. The Y2H screening assays were performed according to the user manual of the BD Matchmaker Two-Hybrid Library Screening Kit (Clontech) using a kiwifruit cDNA library (Liu et al. 2022). For the Y2H assay, the CDS of *AceMYB102* was amplified from the cDNA library and inserted as *EcoRI/BamHI* fragments into the pGADT7 vector containing an activation domain (AD) to generate the prey vector (AceMYB102-AD). AceMYB102-AD was transformed into Y2H gold yeast strain

harboring AcePosF21^{N}-BD. Positively co-transformed cells were selected on dropout medium deficient in Leu and Trp (SD/-Leu/-Trp) and further screened on SD/-Leu/-Trp/-His/-Ade dropout medium, then cultured at 30 °C for 3 d. Positive interactions were identified as blue colonies when grown on media containing X-α-gal (40 μg/mL). Primers of Y2H assay were listed in Supplemental Table S3.

Electromobility shift assay (EMSAs)

The CDS of *AcePosF21* was recombined clone as *BamHI*/*EcoRI* fragments into pET32a vector containing 6×His both in N-terminal and C-terminal by homologous recombination and then transformed into *Escherichia coli* BL21 (DE3) competent cells (TransGen, Beijing, China) to produce recombinant AcePosF21-His protein. Extraction and purification of the protein were based on the methods previously described (Liu et al. 2022). The purified AcePosF21-His fusion protein and the biotin-labeled DNA probes or competitor and mutant probes (Supplemental Table S3) were used for EMSA. The assay was performed using the EMSA Kit (Beyotime, Shang, China) according to the manufacturer's instructions. Photos were captured using a multifunctional imaging system (FluorChem R, Proteinsimple, USA).

Dual-luciferase (dual-LUC) assays

For dual-LUC assay, the promoter regions (fragment upstream from the translational start site) of *AceGGP3* (2.6-kb) and *AcePosF21* (2.1-kb) were amplified from the DNA of kiwifruit and ligated into pGreenII-0800-LUC vector which was linearized by *KpnI* and *HindIII*, to generate *AceGGP3*::*LUC* and AcePosF21::*LUC* reporter constructs, respectively. AcePosF21 was delivered as an effector by overexpression using *AcePosF21* inserted in an overexpression vector (POE-3×Flag-DN; expression driven by 35S promoter) as the effector. The reporter and effector were transformed into *A. tumefaciens* strain GV3101 harboring the pSoup helper vector (Hellens et al. 2005), and mixed reporter and effector in a 1:5 ratio (v/v) and co-infiltrated into 4 wk old *N. benthamiana* leaves with infiltration buffer as described previously (Gao et al. 2020). The injected *N. benthamiana* plants were kept in the dark for 12 h and then for 2 d in 16 h light/8 h dark at 23 °C. The promoter activities were determined by the ratio of REN/LUC using a Dual-luciferase Kit (TransGen, Beijing, China) with a Chemiluminescence Imaging System (Clinx, Shanghai, China).

Chromatin immunoprecipitation (ChIP)—qPCR assay

ChIP-qPCR assay was performed as previously described (Li et al. 2019a, 2019b). The *35S::AcePosF21*-FLAG transgenic and wild-type kiwifruit calli (about 1 g) were cross-linked in 1% formaldehyde for 10 min, following stop cross-linked by 0.125 M glycine. Then the nuclei were isolated and the chromatin was sonicated to an average size of 200–1000 bp using an ultrasonic crushing apparatus (Scientz-IID, Ningbo, China). The protein-DNA complexes were immunoprecipitated by a mouse FLAG antibody (AF2852, Beyotime, China). After elution and reverse cross-linking, the enriched DNA was purified for qPCR. Primers used for ChIP assays are listed in Supplemental Table S3.

Histochemical assay of GUS activity

For β-glucuronidase (GUS) activity and GUS histochemical staining assay, the promoter regions of *AceGGP3* and *AcePosF21* were inserted as *KpnI*/*AscI* fragments into the pMDC162-GUS vector, to produce *AceGGP3*::*GUS* and *AcePosF21*::*GUS* reporter constructs, respectively. Reporter constructs were transformed into the *A. tumefaciens* strain EHA105, then infected into the kiwifruit to obtain transgenic lines, respectively (Liu et al. 2018a, 2018b; Yu et al. 2019). The positive transgenic lines were treated with cold stress (4 °C for 9 h) or at room temperature (25 °C for 9 h), then GUS activity was measured as previously described (Zhang et al. 2020). The GUS histochemical staining assay was performed as previous methods (Zhao et al. 2020; Wu et al. 2022). Transgenic calli were incubated in X-Gluc solution for 12 h at 37 °C. After being fixed in 1% glutaraldehyde at 15 °C for 1 h, the chlorophyll of calli was removed by 50% to 75% to 95% to 50% (v/v) ethanol, and then the calli were photographed.

Subcellular localization assays

The CDS of *AcePosF21* and *AceMYB102* were cloned as *BamHI*/*NcoI* fragments into pFGC-eYFP vector to obtain AcePosF21-YFP and AceMYB102-YFP, then transformed into *A. tumefaciens* strain GV3101, and then injected into *N. benthamiana* leaves as previously described (Gao et al. 2020). The transformed *N. benthamiana* leaves were treated with DAPI, and then fluorescence was observed by a Confocal Microscopy (Leica TCS-SP8). Its excitation wavelength of the signal is 510 nm (YFP) or 488 nm (DAPI), and its emission wavelength is 520 to 560 nm (YFP) or 490 to 540 nm (DAPI), with a 10.0% intensity.

Pull-down assays

The CDS of *AceMYB102* was cloned as *BamHI*/*EcoRI* fragments into pGEX-4 T vector, which contains a glutathione-S-transferase (GST) tag by homologous recombination, to generate recombinant vectors and introduced into BL21 (DE3) competent cells to produce AceMYB102-GST fuzed protein, which was purified according to the previously described method (Xu 2020). The pull-down assay for AceMYB102-GST and AcePosF21-His fuzed protein was carried out as described (Liu et al. 2022).

Bimolecular fluorescence complementation (BiFC) assays

For BiFC assay, the CDS of *AcePosF21* and *AceMYB102* were fuzed as *KpnI*/*SalI* fragments with N-terminal YFP ($_{N}$YFP) in pSPYNE-35S vector and with C-terminal YFP ($_{C}$YFP) in pSPYCE-35S vector to produce AcePosF21-$_{N}$YFP and AceMYB102-$_{C}$YFP, then introduced into *A. tumefaciens* strain GV3101. The AcePosF21-$_{N}$YFP and AceMYB102-$_{C}$YFP vectors were co-transformed (1:1, v/v) into onion

epidermal cells with infiltration buffer (Zhu et al. 2020). After 36 to 48 h infiltrated, YFP fluorescence was detected using a Confocal Microscopy (Leica TCS-SP8). Both signals have an excitation wavelength of 510 nanometers (YFP) or 488 nanometers (DAPI), and an emission wavelength of 520 to 560 nanometers (YFP) or 490 to 540 nanometers (DAPI), with a 10.0% intensity.

Luciferase complementation assays

The luciferase complementation assays were performed using previously described vectors (Chen et al. 2008). The CDS of *AcePosF21* and *AceMYB102* were fuzed as *BamHI*/*KpnI* fragments into pCAMBIA1300-nLUC and pCAMBIA1300-cLUC vectors, respectively, and transformed into *A. tumefaciens* strain GV3101. The *A. tumefaciens* strain carrying AcePosF21- nLUC and AceMYB102- cLUC were mixed in a 1:1 ratio (v/v) and injected into *N. benthamiana* leaves. Plants were incubated in dark for 12 h and then moved to long-day conditions at 23 °C for 2 to 3 d. Observation of luciferase activity was performed as previously described (Liu et al. 2022).

Physiological measurement and histochemical staining

For physiological analysis, the wild-type and transgenic calli of kiwifruit were treated at 25 °C and 4 °C for 6 h. The electrolyte leakage (EL) and malondialdehyde (MDA) contents were determined as previously described (Hu et al. 2020). Proline (Pro), hydrogen peroxide (H_2O_2), and superoxide radical ($O_2^{\cdot-}$) contents were measured using a Proline (Pro) content detection kit, plant peroxide staining solution kit (DAB method), and plant superoxide anion staining solution kit (NBT method) (Solarbio, Beijing, China) following the manufacturer protocol. Histochemical staining of H_2O_2 and $O_2^{\cdot-}$ was conducted with 3,3-diaminobenzidine tetrahydrochloride (DAB) and nitrogen blue tetrazolium (NBT), respectively (Servicebio, Wuhan, China). Determination of ROS content was performed following the manufacturer protocol of a Reactive Oxygen Species Assay (Servicebio, Wuhan, China).

Statistical analysis

For statistical analyses, a minimum of three biological or experimental replicates was used. Significant differences were detected by *t*-test using GraphPad 8.0 software (*$P < 0.05$; **$P < 0.01$; and ***$P < 0.001$). In the figures, the different letters above the bars represent significance groupings ($P < 0.05$) as analyzed by ANOVA using SPSS v20 (IBM Corp., Armonk, NY, USA), and error bars represent standard deviations.

Accession numbers

Sequence data from this article can be found in the GenBank/EMBL data libraries under accession numbers were listed in Supplemental Table S2.

Acknowledgments

The authors would like to thank Xin Haiping, Wang Songhu, Wu Rongmei, Zhou Hui, and the referees for their comments and suggestions, Gao Lei, Li Yeguang, Wen Xiaobin, Lv shiyou, and Jiang Hongsheng for the plant collections.

Supplemental data

The following materials are available in the online version of this article.

Supplemental Figure S1. RT-qPCR analysis of AceGGP3 expression level of transgenic lines.

Supplemental Figure S2. Histochemical staining and fresh weight of *AceGGP3* transgenic kiwifruit calli.

Supplemental Figure S3. Exogenous AsA can protect against damage caused by ROS on kiwifruit.

Supplemental Figure S4. PCA and comparison of differentially expressed genes of kiwifruit calli at RT and COLD treatment for 6 h.

Supplemental Figure S5. AsA accumulation is induced by cold treatment in kiwifruit (*A. eriantha*) fruits.

Supplemental Figure S6. Identification of the transgenic kiwifruit calli which were used for GUS activity assay.

Supplemental Figure S7. Dual-LUC assay analysis of the LUC/REN activity of the *AceGGP3* promoter.

Supplemental Figure S8. Phylogenetic analysis of the evolutionary relationship of *PosF21* and its homologous genes in plant species.

Supplemental Figure S9. Subcellular localization of AcePosF21 protein.

Supplemental Figure S10. Transcriptional activity analysis of AcePosF21.

Supplemental Figure S11. RT-qPCR analysis of *AcePosF21* in kiwi fruits after being treated at 4 °C for 0 h, 2 h, 6 h, 12 h, 1 d, and 3 d.

Supplemental Figure S12. Dual-LUC assay analysis of the LUC/REN activity of *AcePosF21* promoter.

Supplemental Figure S13. SDS polyacrylamide gel electrophoresis detected the protein of AcePosF21-HIS, and AceMYB102-GST protein was successfully expressed and extracted.

Supplemental Figure S14. *AcePosF21* positively regulates AsA accumulation in kiwifruit calli.

Supplemental Figure S15. Protein sequence alignment of wild-type and *AcePosF21*-editing transgenic lines of kiwifruit.

Supplemental Figure S16. Histochemical staining and fresh weight of *AcePosF21* transgenic kiwifruit calli.

Supplemental Figure S17. Phylogenetic analysis of the evolutionary relationship of *MYB102* among plant species.

Supplemental Figure S18. Subcellular localization of AceMYB102 protein.

Supplemental Figure S19. Transcriptional activity analysis of AceMYB102.

Supplemental Figure S20. Transiently expressed *AcePosF21* and *AceMYB102* in kiwifruit calli.

Supplemental Figure S21. RT-qPCR analysis of *AceMYB102* in fruits and calli of kiwifruit after being treated at 4 °C for 0 h, 2 h, 6 h, 12 h, 1 d, and 3 d.

Supplemental Figure S22. Histochemical staining of *AcePosF21* and *AceMYB102* of transient expression of kiwifruit calli.

Supplemental Table S1. Summary statistics of total reads, reads quality, and mapped rate in the calli transcriptomes of kiwifruit.

Supplemental Table S2. The GenBank accession numbers were used in this study.

Supplemental Table S3. Sequences of primers and other oligonucleotides were used in this study.

Funding

This project was supported by the Strategic Priority Research Program of the Chinese Academy of Sciences (XDA24030404), Foundation of Hubei Hongshan Laboratory (2021HSZD017), the National Key R&D Program of China (2019YFD1000201, 2019YFD1000800), Youth Innovation Promotion Association of the Chinese Academy of Sciences (2018376), and National Crop Phenomics Research (Shennong) Facility Project (2021AFB002).

Conflict of interest statement. The authors declare that they have no competing interests.

Data availability

The sequence data of RNA-seq that support the findings of this study can be obtained from GenBank of NCBI (https://www.ncbi.nlm.nih.gov/) under accession no. PRJNA861080.

References

Agami R. Applications of ascorbic acid or proline increase resistance to salt stress in barley seedlings. Biol Plantarum. 2014:**58**(2): 341–347. https://doi.org/10.1007/s10535-014-0392-y

Agarwal P, Baranwal VK, Khurana P. Genome-wide analysis of bZIP transcription factors in wheat and functional characterization of a TabZIP under abiotic stress. Sci Rep. 2019:**9**(1): 4608. https://doi.org/10.1038/s41598-019-40659-7

An JP, Li R, Qu FJ, You CX, Wang XF, Hao YJ. An apple NAC transcription factor negatively regulates cold tolerance via CBF-dependent pathway. J Plant Physiol. 2018a:**221**: 74–80. https://doi.org/10.1016/j.jplph.2017.12.009

An JP, Yao JF, Xu RR, You CX, Wang XF, Hao YJ. Apple bZIP transcription factor MdbZIP44 regulates abscisic acid-promoted anthocyanin accumulation. Plant Cell Environ. 2018b:**41**(11): 2678–2692. https://doi.org/10.1111/pce.13393

Andrews JE, Roberts DWA. Association between ascorbic acid concentrarion and cold hardening in young winter wheat seedings. Can J Bot. 1961:**39**(3): 503–512. https://doi.org/10.1139/b61-039

Anjum NA, Gill SS, Gill R, Hasanuzzaman M, Duarte AC, Pereira E, Ahmad I, Tuteja R, Tuteja N. Metal/metalloid stress tolerance in plants: role of ascorbate, its redox couple, and associated enzymes. Protoplasma. 2014:**251**(6): 1265–1283. https://doi.org/10.1007/s00709-014-0636-x

Bemer M, van Dijk ADJ, Immink RGH, Angenent GC. Cross-family transcription factor interactions: an additional layer of gene regulation. Trends Plant Sci. 2017:**22**(1): 66–80. https://doi.org/10.1016/j.tplants.2016.10.007

Bulley SM, Cooney JM, Laing WA. Elevating ascorbate in *Arabidopsis* stimulates the production of abscisic acid, phaseic acid, and to a lesser extent auxin (IAA) and jasmonates, resulting in increased expression of *DHAR1* and multiple transcription factors associated with abiotic stress tolerance. Int J Mol Sci. 2021:**22**(13): 6743. https://doi.org/10.3390/ijms22136743

Bulley SM, Laing WA. The regulation of ascorbate biosynthesis. Curr Opin Plant Biol. 2016:**33**: 15–22. https://doi.org/10.1016/j.pbi.2016.04.010

Bybordi A. Effect of ascorbic acid and silicium on photosynthesis, antioxidant enzyme activity, and fatty acid contents in canola exposure to salt stress. J Integr Agric. 2012:**11**(10): 1610–1620. https://doi.org/10.1016/S2095-3119(12)60164-6

Cai X, Zhang C, Ye J, Hu T, Ye Z, Li H, Zhang Y. Ectopic expression of *FaGalUR* leads to ascorbate accumulation with enhanced oxidative stress, cold, and salt tolerance in tomato. Plant Growth Regul. 2015:**76**(2): 187–197. https://doi.org/10.1007/s10725-014-9988-7

Cao J, Wang C, Hao N, Fujiwara T, Wu T. Endoplasmic reticulum stress and reactive oxygen species in plants. Antioxidants. 2022:**11**(7): 1240. https://doi.org/10.3390/antiox11071240

Chen H, Zou Y, Shang Y, Lin H, Wang Y, Cai R, Tang X, Zhou JM. Firefly luciferase complementation imaging assay for protein-protein interactions in plants. Plant Physiol. 2008:**146**(2): 368–376. https://doi.org/10.1104/pp.107.111740

Coffel E, Horton RM, De Sherbinin AM (2016) Climate Change and the Frequency of Simultaneous Extreme Heat Events. In Agu fall meeting

Conklin PL, Williams EH, Last RL. Environmental stress sensitivity of an ascorbic acid-deficient *Arabidopsis* mutant. Proc Natl Acad Sci USA. 1996:**93**(18): 9970–9974. https://doi.org/10.1073/pnas.93.18.9970

Dahro B, Wang Y, Khan M, Zhang Y, Fang T, Ming R, Li C, Liu JH. Two AT-hook proteins regulate A/NINV7 expression to modulate sucrose catabolism for cold tolerance in *Poncirus trifoliata*. New Phytol. 2022:**235**(6): 2331–2349. https://doi.org/10.1111/nph.18304

Doru A, Akirlar H. Effects of leaf age on chlorophyll fluorescence and antioxidant enzymes activity in winter rapeseed leaves under cold acclimation conditions. Braz J Bot. 2020:**43**(1): 11–20. https://doi.org/10.1007/s40415-020-00577-9

Elkelish A, Qari SH, Mazrou YS, Abdelaal KA, Hafez YM, Abu-Elsaoud AM, Batiha GE-S, El-Esawi MA, El Nahhas N. Exogenous ascorbic acid induced chilling tolerance in tomato plants through modulating metabolism, osmolytes, antioxidants, and transcriptional regulation of catalase and heat shock proteins. Plants. 2020:**9**(4): 431. https://doi.org/10.3390/plants9040431

Fenech M, Amorim-Silva V, Esteban Del Valle A, Arnaud D, Ruiz-Lopez N, Castillo AG, Smirnoff N, Botella MA. The role of GDP-l-galactose phosphorylase in the control of ascorbate biosynthesis. Plant Physiol. 2021:**185**(4): 1574–1594. https://doi.org/10.1093/plphys/kiab010

Fujita Y, Fujita M, Shinozaki K, Yamaguchi-Shinozaki K. ABA-mediated transcriptional regulation in response to osmotic stress in plants. J Plant Res. 2011:**124**(4): 509–525. https://doi.org/10.1007/s10265-011-0412-3

Gao Y, Wei W, Fan Z, Zhao X, Zhang Y, Jing Y, Zhu B, Zhu H, Shan W, Chen J, et al. Re-evaluation of the nor mutation and the role of the NAC-NOR transcription factor in tomato fruit ripening. J Exp Bot. 2020:**71**(12): 3560–3574. https://doi.org/10.1093/jxb/eraa131

Geng J, Liu JH. The transcription factor CsbHLH18 of sweet orange functions in modulation of cold tolerance and homeostasis of reactive oxygen species by regulating the antioxidant gene. J Exp Bot. 2018:**69**(10): 2677–2692. https://doi.org/10.1093/jxb/ery065

Gietz RD, Schiestl RH. High-efficiency yeast transformation using the LiAc/SS carrier DNA/PEG method. Nat Protoc. 2007:**2**(1): 31–34. https://doi.org/10.1038/nprot.2007.13

Hassani D, Fu X, Shen Q, Khalid M, Rose JKC, Tang K. Parallel transcriptional regulation of artemisinin and flavonoid biosynthesis. Trends Plant Sci. 2020:**25**(5): 466–476. https://doi.org/10.1016/j.tplants.2020.01.001

Hellens RP, Allan AC, Friel EN, Bolitho K, Grafton K, Templeton MD, Karunairetnam S, Gleave AP, Laing WA. Transient expression vectors for functional genomics, quantification of promoter activity and RNA silencing in plants. Plant Methods. 2005:**1**(1): 13. https://doi.org/10.1186/1746-4811-1-13

Hoermiller II, Funck D, Schönewolf L, May H, Heyer AG. Cytosolic proline is required for basal freezing tolerance in *Arabidopsis*. Plant Cell Environ. 2022:**45**(1): 147–155. https://doi.org/10.1111/pce.14196

Hu Z, Huang X, Amombo E, Liu A, Fan J, Bi A, Ji K, Xin H, Chen L, Fu J. The ethylene responsive factor *CdERF1* from bermudagrass (*Cynodon dactylon*) positively regulates cold tolerance. Plant Sci. 2020:**294**: 110432. https://doi.org/10.1016/j.plantsci.2020.110432

Huang X, Cao L, Fan J, Ma G, Chen L. *CdWRKY2*-mediated sucrose biosynthesis and CBF-signalling pathways coordinately contribute to cold tolerance in bermudagrass. Plant Biotechnol J. 2021:**20**(4): 660–675. https://doi.org/10.1111/pbi.13745

Hwang I, Jung HJ, Park JI, Yang TJ, Nou IS. Transcriptome analysis of newly classified bZIP transcription factors of *Brassica rapa* in cold stress response. Genomics. 2014:**104**(3): 194–202. https://doi.org/10.1016/j.ygeno.2014.07.008

Ito K, Kusano T, Tsutsumi K. A cold-inducible bZIP protein gene in radish root regulated by calcium-and cycloheximide-mediated signals. Plant Sci. 1999:**142**(1): 57–65. https://doi.org/10.1016/S0168-9452(98)00250-7

Laing WA, Bulley S, Wright M, Cooney J, Jensen D, Barraclough D, MacRae E. Highly specific *L-galactose-1-phosphate phosphatase* on the path to ascorbate biosynthesis. Proc Natl Acad Sci USA. 2004:**101**(48): 16976–16981. https://doi.org/10.1073/pnas.0407453101

Laing WA, Martínez-Sánchez M, Wright MA, Bulley SM, Brewster D, Dare AP, Rassam M, Wang D, Storey R, Macknight RC, et al. An upstream open reading frame is essential for feedback regulation of ascorbate biosynthesis in *Arabidopsis*. Plant Cell. 2015:**27**(3): 772–786. https://doi.org/10.1105/tpc.114.133777

Li J, Han G, Sun C, Sui N. Research advances of MYB transcription factors in plant stress resistance and breeding. Plant Signal Behav. 2019a:**14**(8): 1613131. https://doi.org/10.1080/15592324.2019.1613131

Li R, Li L, Liu X, Kim J, Jenks M, Lv S. Diurnal regulation of plant epidermal wax synthesis through antagonistic roles of the transcription factors SPL9 and DEWAX. Plant Cell. 2019b:**31**(11): 2711–2733. https://doi.org/10.1105/tpc.19.00233

Liu X, Chen L, Shi W, Xu X, Li Z, Liu T, He Q, Xie C, Nie B, Song B. Comparative transcriptome reveals distinct starch-sugar interconversion patterns in potato genotypes contrasting for cold-induced sweetening capacity. Food Chem. 2021:**334**: 127550. https://doi.org/10.1016/j.foodchem.2020.127550

Liu Y, Hou J, Wang X, Li T, Majeed U, Hao C, Zhang X. The NAC transcription factor NAC019-A1 is a negative regulator of starch synthesis in wheat developing endosperm. J Exp Bot. 2020:**71**(19): 5794–5807. https://doi.org/10.1093/jxb/eraa333

Liu L, McNeilage RT, Shi LX, Theg SM. A ATP requirement for chloroplast protein import is set by the km for ATP hydrolysis of stromal Hsp70 in *Physcomitrella patens*. Plant Cell. 2014:**26**(3): 1246–1255. https://doi.org/10.1105/tpc.113.121822

Liu C, Ou S, Mao B, Tang J, Wang W, Wang H, Cao S, Schläppi MR, Zhao B, Xiao G, et al. Early selection of bZIP73 facilitated adaptation of japonica rice to cold climates. Nat Commun. 2018a:**9**(1): 3302. https://doi.org/10.1038/s41467-018-05753-w

Liu C, Schläppi MR, Mao B, Wang W, Wang A, Chu C. The bZIP73 transcription factor controls rice cold tolerance at the reproductive stage. Plant Biotechnol J. 2019:**17**(9): 1834–1849. https://doi.org/10.1111/pbi.13104

Liu X, Wu R, Bulley SM, Zhong C, Li D. Kiwifruit MYBS1-like and GBF3 transcription factors influence l-ascorbic acid biosynthesis by activating transcription of *GDP-L-galactose phosphorylase 3*. New Phytol. 2022:**234**(5): 1782–1800. https://doi.org/10.1111/nph.18097

Liu Y, Zhou B, Qi Y, Liu C, Liu Z, Ren X. Biochemical and functional characterization of *AcUFGT3a*, a galactosyltransferase involved in anthocyanin biosynthesis in the red-fleshed kiwifruit (*Actinidia chinensis*). Physiol Plant. 2018b:**162**(4): 409–426. https://doi.org/10.1111/ppl.12655

Lo'Ay A, El-Khateeb A. Antioxidant enzyme activities and exogenous ascorbic acid treatment of 'Williams' banana during long-term cold storage stress. Sci Hortic. 2018:**234**: 210–219. https://doi.org/10.1016/j.scienta.2018.02.038

Lu G, Gao C, Zheng X, Han B. Identification of *OsbZIP72* as a positive regulator of ABA response and drought tolerance in rice. Planta. 2009:**229**(3): 605–615. https://doi.org/10.1007/s00425-008-0857-3

Lukatkin A. Contribution of oxidative stress to the development of cold-induced damage to leaves of chilling-sensitive plants: 1. Reactive oxygen species formation during plant chilling. Russ J Plant Physiol. 2002:**49**(5): 622–627. https://doi.org/10.1023/A:1020232700648

Macknight RC, Laing WA, Bulley SM, Broad RC, Johnson AA, Hellens RP. Increasing ascorbate levels in crops to enhance human nutrition and plant abiotic stress tolerance. Curr Opin Biotechnol. 2017:**44**: 153–160. https://doi.org/10.1016/j.copbio.2017.01.011

Matsko SN. Cell resistance to low temperatures as a function of the vitamin factors. Cell Environ Temp. 1967:66. https://doi.org/10.1016/B978-1-4831-6703-9.50017-2

Melero-Jiménez IJ, Bañares-España E, García-Sánchez MJ, Flores-Moya A. Changes in the growth rate of *Chlamydomonas reinhardtii* under long-term selection by temperature and salinity: acclimation vs. evolution. Sci Total Environ. 2022:**822**: 153467. https://doi.org/10.1016/j.scitotenv.2022.153467

Michniewicz M, Kentzer T. The increase of frost resistance of tomato plants through application of 2-chloroethyl trimethylammonium chloride (CCC). Experientia. 1965:**21**(4): 230–231. https://doi.org/10.1007/BF02141905

Min K, Chen K, Arora R. A metabolomics study of ascorbic acid-induced in situ freezing tolerance in spinach (*Spinacia oleracea* L.). Plant Direct. 2020:**4**(2): e00202. https://doi.org/10.1002/pld3.202

Mittler R, Zandalinas SI, Fichman Y, Van Breusegem F. Reactive oxygen species signalling in plant stress responses. Nat Rev Mol Cell Biol. 2022:**23**(10): 663–679. https://doi.org/10.1038/s41580-022-00499-2

Nadarajah KK. ROS Homeostasis in abiotic stress tolerance in plants. Int J Mol Sci. 2020:**21**(15): 5208. https://doi.org/10.3390/ijms21155208

Noctor G, Foyer CH. ASCORBATE AND GLUTATHIONE: keeping active oxygen under control. Annu Rev Plant Physiol Plant Mol Biol. 1998:**49**(1): 249–279. https://doi.org/10.1146/annurev.arplant.49.1.249

Pavet V, Olmos E, Kiddle G, Mowla S, Kumar S, Antoniw J, Alvarez ME, Foyer CH. Ascorbic acid deficiency activates cell death and disease resistance responses in *Arabidopsis*. Plant Physiol. 2005:**139**(3): 1291–1303. https://doi.org/10.1104/pp.105.067686

Peng T, Zhu X, Duan N, Liu JH. PtrBAM1, a β-amylase-coding gene of *Poncirus trifoliata*, is a CBF regulon member with function in cold tolerance by modulating soluble sugar levels. Plant Cell Environ. 2014:**37**(12): 2754–2767. https://doi.org/10.1111/pce.12384

Raza SH, Shafiq F, Chaudhary M, Khan I. Seed invigoration with water, ascorbic and salicylic acid stimulates development and biochemical characters of okra (*Ablemoschus esculentus*) under normal and saline conditions. Int J Agric Biol. 2013:**15**(3): 486–492. https://www.researchgate.net/publication/236344034

Rivero RM, Ruiz JM, García PC, López-Lefebre LR, Sánchez E, Romero L. Resistance to cold and heat stress: accumulation of phenolic compounds in tomato and watermelon plants. Plant Sci. 2001:**160**(2): 315–321. https://doi.org/10.1016/S0168-9452(00)00395-2

Ruelland E, Vaultier M-N, Zachowski A, Hurry V. Cold signalling and cold acclimation in plants. Adv Bot Res. 2009:**49**: 35–150. https://doi.org/10.1016/S0065-2296(08)00602-2

Sanmartin M, Drogoudi PA, Lyons T, Pateraki I, Barnes J, Kanellis AK. Over-expression of ascorbate oxidase in the apoplast of transgenic tobacco results in altered ascorbate and glutathione redox states and increased sensitivity to ozone. Planta. 2003:**216**(6): 918–928. https://doi.org/10.1007/s00425-002-0944-9

Shafiq S, Akram NA, Ashraf M, Arshad A. Synergistic effects of drought and ascorbic acid on growth, mineral nutrients and oxidative defense system in canola (*Brassica napus* L.) plants. Acta Physiol Plant. 2014:**36**(6): 1539–1553. https://doi.org/10.1007/s11738-014-1530-z

Shekhawat UKS, Ganapathi TR. Transgenic banana plants overexpressing *MusabZIP53* display severe growth retardation with enhanced sucrose and polyphenol oxidase activity. Plant Cell Tiss Org. 2014:**116**(3): 387–402. https://doi.org/10.1007/s11240-013-0414-z

Smirnoff N. Vitamin C: the metabolism and functions of ascorbic acid in plants. Adv Bot. 2011:**59**: 107–177. https://doi.org/10.1016/B978-0-12-385853-5.00003-9

Sun X, Li Y, Cai H, Bai X, Ji W, Ji Z, Zhu Y. *Arabidopsis* bZIP1 transcription factor binding to ABRE cis-element regulates abscisic acid signal transduction. Acta Agron Sin. 2011:**37**(4): 612–619. https://doi.org/10.1016/S1875-2780(11)60016-3

Sun X, Zhang L, Wong DCJ, Wang Y, Zhu Z, Xu G, Wang Q, Li S, Liang Z, Xin H. The ethylene response factor *VaERF092* from Amur grape regulates the transcription factor VaWRKY33, improving cold tolerance. Plant J. 2019:**99**(5): 988–1002. https://doi.org/10.1111/tpj.14378

Suzuki N, Mittler R. Reactive oxygen species and temperature stresses: a delicate balance between signaling and destruction. Physiol Plant. 2006:**126**(1): 45–51. https://doi.org/10.1111/j.0031-9317.2005.00582.x

Tang W, Sun X, Yue J, Tang X, Jiao C, Yang Y, Niu X, Miao M, Zhang D, Huang S, et al. Chromosome-scale genome assembly of kiwifruit *Actinidia eriantha* with single-molecule sequencing and chromatin interaction mapping. Gigascience. 2019:**8**(4): giz027. https://doi.org/10.1093/gigascience/giz027

Wang Q, Shi H, Huang R, Ye R, Luo Y, Guo Z, Lu S. AIR12 Confers cold tolerance through regulation of the CBF cold response pathway and ascorbate homeostasis. Plant Cell Environ. 2021:**44**(5): 1522–1533. https://doi.org/10.1111/pce.14020

Wang Z, Wang S, Li D, Zhang Q, Li L, Zhong C, Liu Y, Huang H. Optimized paired-sgRNA/Cas9 cloning and expression cassette triggers high-efficiency multiplex genome editing in kiwifruit. Plant Biotechnol J. 2018:**16**(8): 1424–1433. https://doi.org/10.1111/pbi.12884

Wheeler GL, Jones MA, Smirnoff N. The biosynthetic pathway of vitamin C in higher plants. Nature. 1998:**393**(6683): 365–369. https://doi.org/10.1038/30728

Wu T, Alizadeh M, Lu B, Cheng J, Hoy R, Bu M, Laqua E, Tang D, He J, Go D, et al. The transcriptional co-repressor *SEED DORMANCY 4-LIKE* (*AtSDR4L*) promotes embryonic-to-vegetative transition in *Arabidopsis thaliana*. J Integr Plant Biol. 2022:**64**(11): 2075–2096. https://doi.org/10.1111/jipb.13360

Xiang Y, Tang N, Du H, Ye H, Xiong L. Characterization of *OsbZIP23* as a key player of the basic leucine zipper transcription factor family for conferring abscisic acid sensitivity and salinity and drought tolerance in rice. Plant Physiol. 2008:**148**(4): 1938–1952. https://doi.org/10.1104/pp.108.128199

Xiao Y, Li Z, Yi P, Hu R, Zhang X, Zhu L. Research progress on response mechanism of transcription factors involved in plant cold stress. Biotechnol Bull. 2018:**34**(12): 1–9. https://doi.org/10.13560/j.cnki.biotech.bull.1985.2018-0240

Xu C. Pull-down and co-immunoprecipitation assays of interacting proteins in plants. Chinese Bull Bot. 2020:**55**(1): 62–68. https://doi.org/10.11983/CBB19143

Ye N, Zhu G, Liu Y, Zhang A, Li Y, Liu R, Shi L, Jia L, Zhang J. Ascorbic acid and reactive oxygen species are involved in the inhibition of seed germination by abscisic acid in rice seeds. J Exp Bot. 2012:**63**(5): 1809–1822. https://doi.org/10.1093/jxb/err336

Yoshida T, Fujita Y, Maruyama K, Mogami J, Todaka D, Shinozaki K, Yamaguchi-Shinozaki K. Four *Arabidopsis*nAREB/ABF transcription factors function predominantly in gene expression downstream of SnRK2 kinases in abscisic acid signalling in response to osmotic stress. Plant Cell Environ. 2015:**38**(1): 35–49. https://doi.org/10.1111/pce.12351

Yu M, Man Y, Wang Y. Light- and temperature-induced expression of an R2R3-MYB gene regulates anthocyanin biosynthesis in red-fleshed kiwifruit. Int J Mol Sci. 2019:**20**(20): 5228. https://doi.org/10.3390/ijms20205228

Zhang C, Liu J, Zhang Y, Cai X, Gong P, Zhang J, Wang T, Li H, Ye Z. Overexpression of *SlGMEs* leads to ascorbate accumulation with enhanced oxidative stress, cold, and salt tolerance in tomato. Plant Cell Rep. 2011:**30**(3): 389–398. https://doi.org/10.1007/s00299-010-0939-0

Zhang Y, Zhou Y, Zhang D, Tang X, Xia X. *PtrWRKY75* overexpression reduces stomatal aperture and improves drought tolerance by salicylic acid- induced reactive oxygen species accumulation in poplar. Environ Exp Bot. 2020:**176**: 104117. https://doi.org/10.1016/j.envexpbot.2020.104117

Zhao XY, Qi CH, Jiang H, Zhong MS, You CX, Li YY, Hao YJ. *MdWRKY15* improves resistance of apple to botryosphaeria dothidea via the salicylic acid-mediated pathway by directly binding the *MdICS1* promoter. J Integr Plant Biol. 2020:**62**(4): 527–543. https://doi.org/10.1111/jipb.12825

Zhu W, Zhou H, Lin F, Zhao X, Jiang Y, Xu D, Deng XW. COLD-REGULATED GENE27 integrates signals from light and the circadian clock to promote hypocotyl growth in *Arabidopsis*. Plant Cell. 2020:**32**(10): 3155–3169. doi:10.1105/tpc.20.00192